Sutural complexity in Late Jurassic ammonites and its relationship with phragmocone size and shape: a multidimensional approach using fractal analysis

JUAN A. PÉREZ-CLAROS, FEDERICO OLÓRIZ AND PAUL PALMQVIST

LETHAIA

Pérez-Claros, J.A., Olóriz, F. & Palmqvist P. 2007: Sutural complexity in Late Jurassic ammonites and its relationship with phragmocone size and shape: a multidimensional approach using fractal analysis. *Lethaia*, Vol. 40, pp. 253–272.

The evolution of intricate septa and complex sutural patterns in cephalopod ammonoids is one of the best documented trends in the fossil record towards increased levels of complexity. Functional interpretation of septal folding is still, however, a matter of controversy. Tentative explanations have been linked to the structural reinforcement of phragmocones, mantle area increase, buoyancy control and even metabolic functions concerning respiration or cameral liquid transport. Here we use fractal analysis in order to estimate suture complexity in a large set ($N = 524$) of Late Jurassic ammonites, and its covariation with phragmocone size, shape and ornamentation. Sutural complexity, estimated by fractal dimension (D_f), is closely related to phragmocone whorl height and the degree of shell involution, while this trend is reversed for tubercle size. On average, specimens from epioceanic habitats display lower D_f values than those inhabiting epicontinental waters. Our results reveal a complex relationship between sutural complexity and morphometric descriptors of phragmocones, indicating that septal folding was more closely related to shell geometry than to bathymetry. In addition, these results fit predictions of a recent model relating sutural complexity to energetic demands of ammonoid metabolism. However, future research should not neglect the implications of phylogenetic legacy as an important source of variability in fractal dimensions. □ *Ammonites, fractals, Late Jurassic, morphometrics, shell morphology, sculpture, suture complexity.*

Juan A. Pérez-Claros [johnny@uma.es] and Paul Palmqvist [ppb@uma.es], Departamento de Ecología y Geología, Facultad de Ciencias, Universidad de Málaga, Campus Universitario de Teatinos, 29071 Málaga, Spain; Federico Olóriz [foloriz@ugr.es], Departamento de Estratigrafía y Palaeontología, Facultad de Ciencias, Universidad de Granada, Campus Universitario de Fuentenueva, 18002 Granada, Spain; *manuscript received on 21/12/2005; manuscript accepted on 21/3/2007.*

The evolutionary history of septal sutures in ammonoid cephalopods illustrates a long-term trend towards higher levels of morphological complexity, which partially results from the temporal replacement of three basic sutural types: (1) the goniatitic type (most lobes undivided, typical of Palaeozoic ammonoids); (2) the ceratitic type (most lobes divided but not the saddles, characteristic of the Triassic); and (3) the ammonitic type (lobes and saddles divided, representative of Jurassic–Cretaceous ammonoids) (Dommergues 1990; Boyajian & Lutz 1992; Saunders & Work 1997; Saunders *et al.* 1999; Allen 2006). There are, however, exceptions to this general pattern, as some Palaeozoic genera exhibit ammonitic sutures, some Triassic ammonoids show goniatitic sutures and some Jurassic and Cretaceous lineages have ceratitic sutures (Arkell *et al.* 1957). In addition, septal folding increased over time in each of these sutural types and became more complex through ontogeny, which reveals the prevalence of peramorphic processes in ammonoid sutural evolution (Landman 1988; Dommergues 1990). Notwithstanding, the mean level of complexity reached by early Cretaceous ammonoids remained quasi-constant until the extinction of the group (Boyajian & Lutz 1992).

Given that a septal suture cannot be simpler than a straight line (i.e. the 'left wall of complexity' *sensu* Gould 1996), the increase in sutural complexity may reflect a diffusion from an initial condition of simple, low-variable sutures through the subsequent generation of higher morphological variability, without implying an increase of fitness (Stanley 1973; Fisher 1986; Gould 1988; Boyajian & Lutz 1992). This hypothesis was, however, refuted by Saunders *et al.* (1999), who concluded that increasing sutural complexity over the first 140 Ma of ammonoid evolution is better described by an active or directed trend than by a passive or diffused one.

After more than 160 years of debate, the interpretation of extreme septal folding in ammonoids is still controversial, as sutural complexity has been tentatively related to a wide spectrum of functions, including: (1) structural reinforcement of phragmocones against the hydrostatic load or the pressure generated by

DOI 10.1111/j.1502-3931.2007.00022.x

predator teeth; (2) area increase for mantle-to-septum joining; (3) a role in buoyancy control; and (4) a metabolic function linked to respiration or cameral liquid transport (for reviews and references, Raup & Stanley 1971; Ward 1981; Saunders & Work 1996, 1997; Olóriz *et al.* 1997, 1999, 2002; Pérez-Claros 1999, 2005; Saunders *et al.* 1999; Lewy 2002; Pérez-Claros *et al.* 2002).

The preservational completeness of the ammonoid fossil record makes it difficult to realize morphometric characterizations of sutural complexity, and the absence of extant relatives hinders functional interpretation. Thus, the interpretation of folded septa must be based on indirect evidence such as the covariation of sutural parameters with the geometry and ornamentation of phragmocones (e.g. see Yacobucci 2004). However, there are no unequivocal interpretations for the entire group of ammonoids, as many observations on the relationship between sutural complexity and phragmocone shape remain contradictory. For example, an increase in sutural complexity appears to be associated with rounded whorl sections in evolute phragmocones (Arkell *et al.* 1957; Bayer 1977; Bayer & McGhee 1984), but some authors maintain that these characters are unrelated (e.g. Kennedy & Cobban 1976; Courville *et al.* 1998) and others even describe an inverse relationship (Buckman 1892; Haas 1942; Westermann 1966; Hewitt & Westermann 1987; Donovan 1994; Olóriz *et al.* 1997, 1999). In addition, the quantification of sutural complexity and phragmocone shape has usually led to inconsistent results for different groups of ammonoids, even when using similar morphometric methodologies. For example, Saunders & Work (1996) found that sutural complexity was unrelated to phragmocone shape in goniatitids, and Saunders (1995) revealed that no significant reduction in either septum thickness or shell thickness accompanied the 100-fold increase in sutural complexity of Palaeozoic ammonoids. However, Saunders & Work (1997) found an unequivocal relationship of sutural complexity with shell coiling and lateral compression in prolecanitids, the 'rootstock' of Mesozoic ammonoids, suggesting a 'phylogenetic overprint' that could, in turn, be used to interpret the latter.

Two basic questions should be addressed when focusing on the evolution of sutural complexity: (1) What is meant by sutural complexity? (2) How should it be quantified? No precise definition has been proposed for a general concept of complexity, as many disparate concepts have been proposed for measuring it, including entropy, information, linguistic syntax, fractals, constructional complexity, and component diversity, among others. According to McShea (1991), a limited consensus exists where morphological or structural complexity, whether it concerns biological systems or not, can be considered a function of component diversity and their uneven distribution within a given system. Such a concept is, however, inconclusive when applied to real objects. For example, given that septal fluting is an iterative, branching process, the constructional complexity of all suture lines is probably almost equal and relatively low. Similarly, the component diversity of sutures also implies low complexity. In general, it is more appropriate to quantify morphological characteristics that are somehow linked to complexity making reference to the method used for complexity level identification.

Sutural complexity in ammonoids has been mathematically characterized using simple parameters, such as the index of sutural complexity introduced by Westermann (1971) and later termed *SCI* by Ward (1980) and *SI* by Saunders (1995). This index is calculated through the division of sutural perimeter by the length of a segment that joins the two extremes of the suture. It has been used in its basic form and also modified to include the count of sutural elements (Saunders 1995). Fourier series have also represented a morphometric tool for ammonoid sutures, as first proposed by Canfield & Anstey (1981), although they can only be used with relatively simple sutures (Lutz & Boyajian 1995). However, Gildner (2003) proposed a variant of this methodology that is applicable to a wider spectrum of sutural lines, and Allen (2006) developed a more robust mathematical approach for analyzing the shape of complex curves, the windowed short-time Fourier transform. These approaches seem to be promising, but further evaluation will be necessary to determine its potential for addressing taxonomical and evolutionary issues. Finally, a third approach based on fractal geometry (Mandelbrot 1983) produces good results in the evaluation of sutural complexity (García-Ruiz *et al.* 1990; Boyajian & Lutz 1992; Lutz & Boyajian 1995; Olóriz & Palmqvist 1995; Olóriz *et al.* 1997, 1999, 2002; Pérez-Claros *et al.* 2002), and is the methodology we have chosen for our case study.

The present paper has two main objectives: (i) to apply a new technique of fractal analysis that enables the mathematical characterization of several features of sutural complexity (Pérez-Claros *et al.* 2002); and (ii) to analyze the covariation of such features with those concerning phragmocone shape, size and ornamentation in a large set of Late Jurassic ammonites.

Material and methods

Characterization of sutural complexity

A fractal object can be defined as a set composed of parts that are identical to the whole (Mandelbrot

1983). This property, called homothety, implies that mathematical fractals are self-similar. Natural objects with some kind of internal homothety (e.g. ammonitic sutures) are not perfect fractals, as their parts (e.g. major saddles and lobes) are not identical to the whole. However, although the exact shape of these objects is not maintained, their degree of complexity remains constant at varying scales of observation, showing statistical self-similarity.

The first estimates of fractal exponents for ammonoid sutures were given by Long (1985). Several authors have since noted the self-similar nature of ammonite suture lines (e.g. Bayer 1985; Damiani 1986; Seilacher 1988; García-Ruiz *et al.* 1990; Lutz & Boyajian 1995; Olóriz & Palmqvist 1995; Olóriz *et al.* 1997, 1999, 2002), something which is less evident in goniatitids and ceratitids.

One of the most important properties of a fractal object is its fractal dimension (D_f), a measure of irregularity or sinuosity comprised between one (the Euclidean dimension for a line) and two (the topological dimension of a surface). Thus, D_f may intuitively be conceived as an estimate of the degree to which the curve departs from a straight line to fill a plane. D_f for mathematical fractals is exclusively determined by generator curve shape. In fractal curves with statistical self-similarity, in which the exact shape of the generator cannot be determined, there are two basic approaches for estimating D_f: (1) Richardson's method, which estimates the perimeter of the analyzed curve using as scale of measurement a set of rulers or straight segments of increasing length; and (2) the box counting method, which uses squares of increasing side length (see details in Olóriz *et al.* 1999).

Mathematical fractals maintain their self-similar nature at any scale of observation. Fractals with statistical self-similarity (e.g. ammonitic sutures) have upper and lower limits above and below which such a property no longer applies. This implies that D_f must be estimated within the range of scales of measurement in which the septal sutures are self-similar. Although this range can be estimated visually (Lutz & Boyajian 1995), here we use a procedure that allows to obtain a more objective value for the lower limit of self-similarity, providing independent estimates of first and second orders of sutural complexity (Pérez-Claros *et al.* 2002). This method is based on the fact that, when the lower limit of self-similarity or 'cut-off' (X_c) is approached due to decreasing step length, the logarithmic graph of ruler size (r) and perimeter length (L) will tend towards a straight line with a null slope, characteristic of non-self-similar objects (Fig. 1A). The value of X_c is determined by the point at which the tangent of the function is parallel to the straight line that joins the extremes of the suture (Fig. 2B). The bilogarithmic graph may be fitted to a power function:

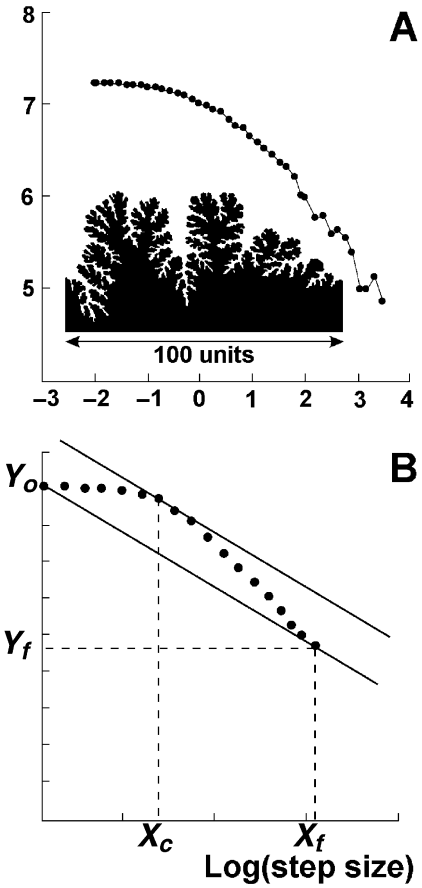

Fig. 1. □A. Bivariate log–log plot of estimated perimeter for a *Holcostephanus (Spiticeras) scriptus* suture relative to the length of the ruler used to measuring it. The graph becomes a line with null slope when the size of the ruler tends toward smaller values. □B. A method for dividing this graph in two consists of finding the value of the point in the measurement scale (x-axis) for which the slope of the curve equals that connecting both extremes of the plot.

$$\log_e(L) = K - a[\log_e(r)]^b, \quad (1)$$

which enables the estimation of X_c. D_f may then be calculated at both sides of X_c using the slope adjusted for each straight line. Only the fractal dimension estimated for the upper range of scales of measurement (D_{f2}) is a real fractal exponent. Lower range values (D_{f1}) indicate, at most, the tendency of the curve to behave as a Euclidean object within the range of ruler sizes analyzed.

X_c measures the point below which there is a loss of self-similarity (i.e. a low value of X_c indicates that the sutures behaves in a self-similar manner at low scales of measurement while a high value informs of an early loss of self-similarity at larger scales). Therefore, X_c may be considered an inverse index of self-similarity,

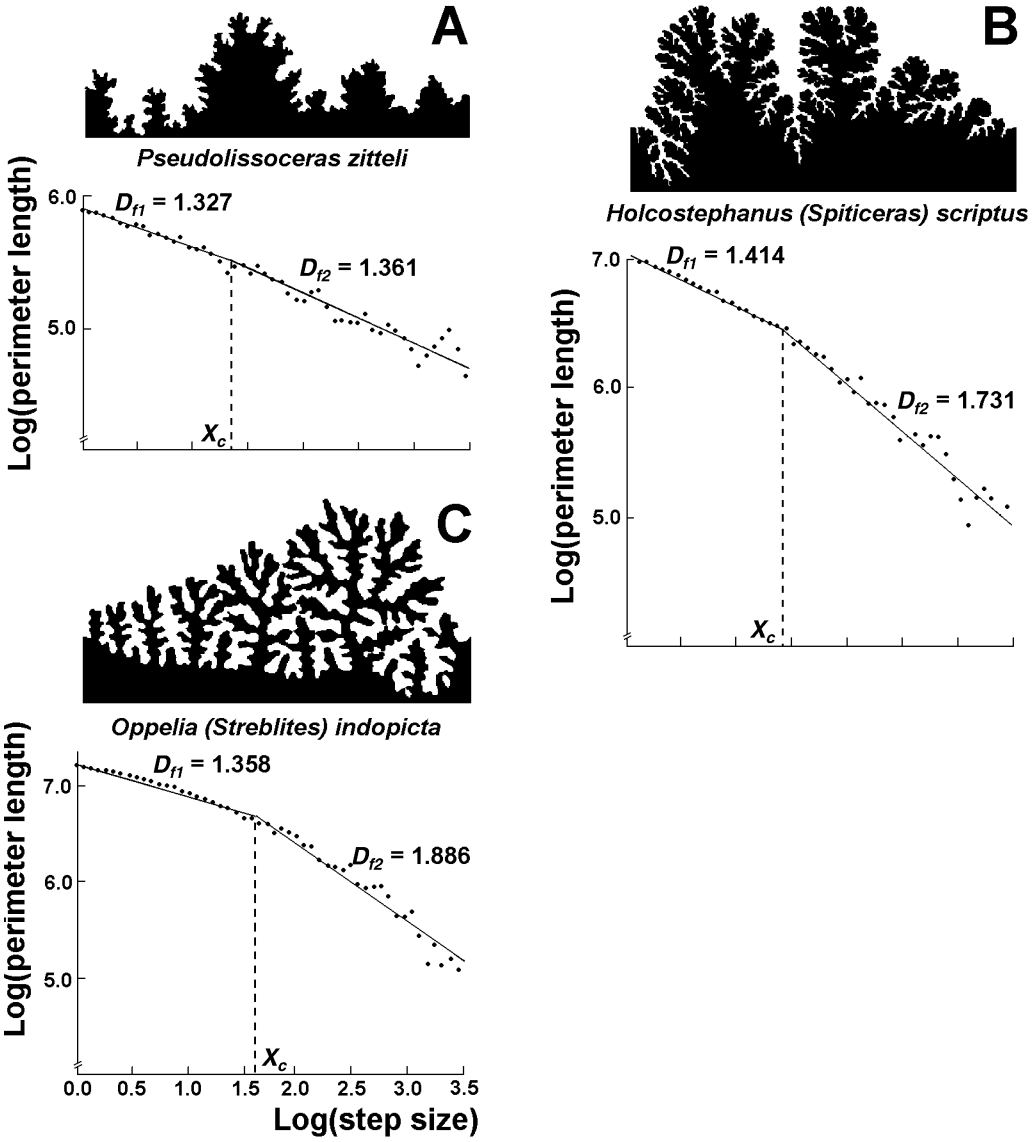

Fig. 2. Three examples of the application of the method shown in Figure 2 for ammonitic sutures: □A. *Pseudolissoceras zitteli*, □B. *Holcostephanus (Spiticeras) scriptus,* and □C. *Oppelia (Streblites) indopicta.* Once the graph has been divided in two parts, fitting independent straight lines to them and adjusting D_f values is straightforward (see text for details).

fully comparable among different sutures, as long as they are analyzed using the same ruler sizes. The sutures must be standardized to an equivalent length between two comparable landmarks (Pérez-Claros *et al.* 2002). The landmarks in this study are the medial point of the ventral saddle and the point where the suture is overlapped by the previous whorl. Both landmarks may be considered equivalent among different sutures, although only the first is, *sensu stricto*, a homologous point. According to Pérez-Claros *et al.* (2002), if the suture maintains its fractal nature over the range of scales of measurement (thus, the parameter 'b' of eq. (1) tends to approach the value 1), then the value of X_c is constant and equals:

$$X_c = X_f/a, \quad (2)$$

where X_f is the logarithm of the maximum ruler size used and a is the base of this logarithm. In this article, $X_f = \log_e(2^5)$ and $a = e$. This gives an expected value of $X_c = 1.275$ for the lower limit of self-similarity when the fractal nature of sutures is maintained throughout the ruler-size range (i.e. $\log_e(32)/e$).

This method was applied to 524 sutures from well-preserved, mature specimens of worldwide Late Jurassic planispiral ammonites taken from published literature, including Phylloceratina ($N = 20$), Lytoceratina ($N = 6$) and Ammonitina ($N = 499$) (for details and references, see Olóriz *et al.* 1997; Pérez-Claros

1999). In each specimen a single suture line was taken into account. These sutures satisfy the following requirements: (1) they belong to adult individuals; (2) they are complete between the middle point of the siphonal lobe and the point of overlap with the previous whorl; and (3) they show no evidence of erosion. Sutures were enlarged enough to be accurately digitized in (x,y) coordinates using a Calcomp digitizing tablet, which enables a precision of 0.1 mm, and thus the use of 18 points per centimetre of digitized perimeter on average. Sutures were standardized to a length of 100 arbitrary units between both extremes (Pérez-Claros *et al.* 2002) and were then analyzed using Richardson's method, with 51 ruler lengths of between 2^0 (i.e. 1) and 2^5 (i.e. approximately a third of the length of the line that joins both suture ends) through exponential increases of $2^{0.1}$ units. The last rule of measurement for each series was counted when the distance between the last point of anchorage for the ruler and the end of the suture was greater than 50% of the ruler length. This procedure was applied to each suture starting from both ends. Averaging of the values obtained for the adjusted parameters was then carried out.

The method allows quantification of both the range of self-similarity and the level of septal suture complexity and provides results that may be interpreted in geometric terms. Figure 2 shows three examples of sutures in which important differences can be seen in the range of self-similarity and the degree of complexity, at both scales of measurement. The sutures represented in Figure 2A, B show similar X_c values (i.e. the range of scales where they behave as fractals is approximately the same), although the second suture is more complex at both scales of measurement, as reflected in higher values of D_{f1} and D_{f2}. Sutures in Figure 2B, C exemplify high complexity at large scales of measurement, reflected in high D_{f2} values. However, although the suture of Figure 2C nearly fills a plane, it shows lower complexity at small scales and a narrower range of self-similarity than the one represented in Figure 2B, as revealed by its higher X_c value and lower D_{f1} value.

Given that the sutures were standardized to a length of 100 units between their ends, the value of K in equation (1) obtained in the statistical fitting of the bilogarithmic plot is related to the index of sutural complexity (*SCI*) by the following equation:

$$SCI = e^K/100, \quad (3)$$

and may also be used as a morphometric descriptor of the sutures.

Other sutural indexes were also obtained (Fig. 3), including the relative sutural amplitude (S_a) and the maximum relative height of the lobes or saddles (S_h) (Batt 1986).

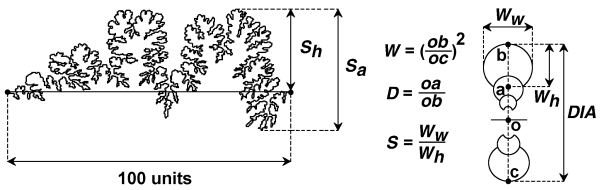

Fig. 3. Standardized sutural amplitude and height, and description of several variables related to phragmocone size and shape. After the line connecting both suture extremes has been set at 100 units, S_a is defined as the maximal perpendicular distance found above and below the connecting line, and S_h is estimated in the same way but only for the longer segment defined by the cut of the connecting line, which measures the height of the saddle-ward (i.e. aperture-ward) portion of the suture. *W*: whorl expansion rate. *D*: distance of generating curve from coiling axis. *S*: whorl shape. P_{dia}: phragmocone diameter. W_h: whorl height. W_w: whorl width. P_{dia} and W_h were measured at the level of the suture analyzed.

Characterization of phragmocone size and shape

The morphometric characterization of phragmocones was carried out considering: (1) size; (2) degree of whorl coiling; and (3) shape of whorl section in the last whorl. The database included photographs and accurate drawings of whorl sections for 494 specimens, while estimates of phragmocone size were available in 460 cases.

Phragmocone size (Fig. 3) was estimated using whorl height (W_h) and phragmocone diameter (P_{dia}). These variables were measured in millimetres at the level of the digitized sutures. Since planispiral ammonoid growth is reasonably well described by the logarithmic spiral model (Raup 1967; Okamoto 1996), W_h and P_{dia} were logarithmically transformed, allowing these estimates of phragmocone size to increase linearly with whorl number.

Whorl coiling was characterized using the model proposed by Raup (1966). This model considers the position of the generative curve and its displacement around the coiling axis (parameters *D* and *W* in Fig. 3, respectively). Although there are more sophisticated models (e.g. Illert 1987, 1989; Okamoto 1984, 1986, 1988; Ackerly 1987, 1989; Stone 1995; Rice 1998), the one originally proposed by Raup possesses the following advantages: (1) ease of obtaining the value of the parameters in the phragmocones; (2) ease of interpretation; and (3) good fit between simulated and real morphologies. In addition, the use of this model enables the comparison of our results and previously published data.

Another important feature of phragmocones is the cross-sectional shape of their outer whorls. Raup

(1966, 1967) simplified this shape by considering it an ellipse, described by a parameter *S* that is defined as the ratio of maximum width to maximum height of whorl section (Fig. 3). Although this index is appropriate for characterizing most whorl sections, there are morphologies displaying identical *S* values but differential flank curvature.

Several methods have been developed for the analysis of shape and curvature of biological outlines, including different modalities of Fourier analysis (e.g. open or closed outlines, polar radii and elliptic analysis; for a comprehensive review, see Rohlf 1990; Palmqvist *et al.* 1996), eigenshape analysis (Lohmann 1983; Lohmann & Schweitzer 1990; MacLeod 1999), and methods for the estimation of median axes of symmetry or line skeletons (Straney 1990). We have used here Fourier analysis of closed outlines following the polar radius approach (Ehrlich & Weinberg 1970; Palmqvist *et al.* 1996). Fourier series for closed outlines consist of equations incorporating sines and cosines that can describe and reproduce any bi-dimensional figure in which the radii from its centre of gravity intercept the outline only once. The shape of the outline is estimated from the following equation, which fits the expansion of a radius *R* running from the centroid of the figure as a function of the angle of rotation (θ) in a system of polar coordinates:

$$R(\theta) = R_o\left[1 + \sum_{n=1}^{\infty} A_n \cos(n\theta) + \sum_{n=1}^{\infty} B_n \sin(n\theta)\right] \quad (4)$$

an equation that is normally used in the following transformation:

$$R(\theta) = R_o\left[1 + \sum_{n=1}^{\infty} H_n \cos(n\theta - P_n)\right] \quad (5)$$

$$\text{with } H_n = (A_n^2 + B_n^2)^{1/2} \text{ and } P_n = \arctan(B_n/A_n), \quad (6)$$

where R_o is the radius of a circumference with an area equivalent to that of the outline analyzed, *n* indicates the harmonic order, H_n is the harmonic amplitude of the *nth*-order harmonic, and P_n is its phase angle.

This analysis allows the outline to be split into its geometrical components, regardless of size and without needing to take homologous points. The amplitudes of low-order harmonics measure the overall geometric components of shape (e.g. the second and third harmonics estimate the contribution of a two-foil and a three-foil, respectively, thus measuring the degree of elongation and triangularity of the outline), whereas higher-order harmonics involve details of increasingly fine-scaled sculpture (e.g. the *nth*-order harmonic amplitude represents the shape contribution of an *n*-leaved clover). The amplitude of the first harmonic measures the error of adjustment.

Given that the equation used for describing $R(\theta)$ is single-valued, Fourier analysis of closed outlines cannot be applied to morphologies in which a radius from the centroid intersects the periphery more than once. Hence, it is not adequate for analyzing the shape of whorl sections in involute ammonoids (i.e. $WD < 1$) whose final whorl partially covers the preceding ones. The morphometric analysis of this specific region of the shell, which is an open outline, requires closing the dorsal periphery of the whorl with a straight line (Fig. 4).

Figure 4 illustrates two computer-generated simulations of ammonite whorl cross-sections obtained by incorporating successive harmonics into the Fourier series. Although a relatively high number of harmonics (10) is necessary for a thorough characterization of a whorl cross-section, in both cases the major geometric features are appropriately described by the first five harmonics.

Another significant aspect of Fourier analysis is the relative orientation of the harmonics in the outline, which is reflected in their phase angles. The phase angle, divided by the harmonic order, measures

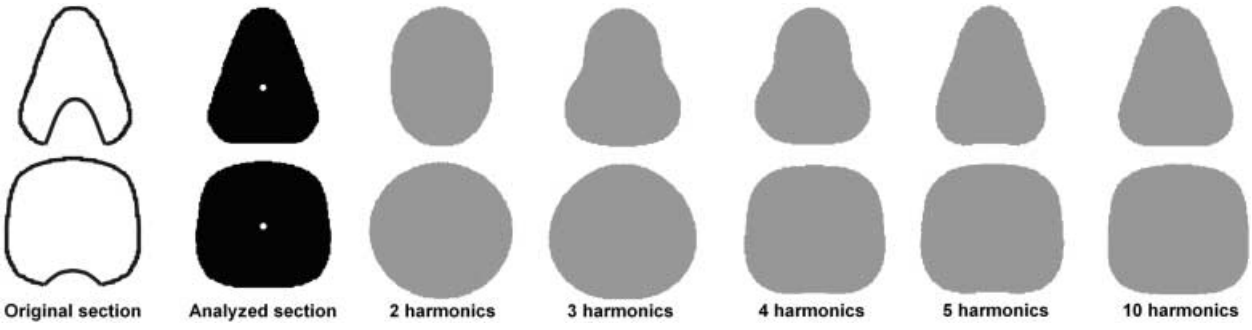

Fig. 4. Simulations of whorl-section outlines using an increasing number of harmonics for two different morphologies from the analyzed dataset. Numbers refer to the harmonic order used (e.g. 2 for elongation, 3 for triangularity, and 4 for quadrangularity).

the orientation of the first harmonic lobe. Given that all sections were situated with the symmetry axis vertically oriented in the digitizing tablet, these values are then comparable among the specimens analyzed. The use of phase angles is not, however, problem-free (Palmqvist 1989), since two similar outlines with a similarly oriented harmonic may display highly distinct values for their phase angles. This occurs when the orientation of the first lobe swings around the axis of symmetry in figures that do not show a perfect bilateral symmetry. In order to solve this problem, the phase angle was transformed as:

$$P_n^{\star} = \mathrm{ABS}[(360°/n) - (P_n/n)] + 360°/n, \qquad (7)$$

where *ABS* is the absolute value, n is the harmonic order and P_n is the phase angle in hexadecimal degrees.

Only the phase angles of the second and fourth harmonics were used as morphometric variables in our study, because these are the harmonics that show greater variability in the sample. Where the second harmonic is important in the outline, $P_2^{\star}$ may take values close to 180° or 90°, which depends on whether the section is depressed or laterally compressed. When the contribution of the fourth harmonic is high, the phase angle $P_4^{\star}$ takes values of around 45° (quadrangular sections) or 90° (rhomboidal sections). Quadrangular sections usually show relatively low amplitudes for the fourth harmonic, although this is the only harmonic that provides a significant contribution to the description of their shape. Thus the fourth harmonic amplitude is scaled by the sum of the amplitudes for the other harmonics (Pérez-Claros 1999):

$$H_{4r} = H_4 / \sum_{i=1}^{5} H_i \qquad (8)$$

In addition, the circularity index C_2 (Davis 1986) was estimated for each whorl section, using the following equation:

$$C_2 = 4\pi A / P^2, \qquad (9)$$

where A is the cross-sectional area and P is whorl perimeter, both calculated before the outline is closed.

Ornamental features with elusive morphometric characterization, i.e. the occurrence and development of tubercles (*TUB*) and ribs (*RIB*), were approached using variables in ordinal scale. For both features the following codes were used: (1) absence of element; (2) small- to medium-sized element; and (3) large-sized element. It is worth noting that the qualitative categories 'small to medium' and 'large' make reference to the relative size or density of ribs and tubercles (i.e. percentage of the surface of the phragmocone covered by these elements, estimated visually). Other ornamental elements (e.g. furrows and constrictions) unrelated to sutural complexity (Olóriz & Palmqvist 1995) were not considered.

Finally, a qualitative palaeoecologically related variable (*ECO*) was used to take into account major environments and/or ecological tolerance: (1) neritics; (2) ubiquitous; and (3) epioceanics. Considering dimensions of the shell and siphuncle in ammonoids, Chamberlain *et al.* (1981) concluded that the water flux through the siphuncle would not allow for a long-lasting buoyancy of the carcass, as in *Nautilus*. Therefore, transportation of ammonoid shells far from their home range would seem unlikely or, at least, uncommon for most ammonites. Although the results of Chamberlain *et al.* (1981) indicate coherence between the eco-sedimentary environment and the lithostratigraphic record, at least for medium-sized Mesozoic ammonoids, such coherence would be more informative of habitat distance from the shoreline than of habitat depth. In fact, no direct relationship can be proven among distance from the shoreline and depth, except for ramps, especially in structured palaeomargins (e.g. in central-western Tethys). Moreover, the combined effects of physico-chemical properties of water and depth of death are usually beyond empirical control, although they have become crucial for the interpretation of particular cases (for an extended discussion of this topic, see Maeda & Seilacher 1996).

Results

Table 1 shows several statistics for the morphometric descriptors, the correlations among these variables (lower triangular matrix) and their level of statistical significance (upper triangular matrix). Spearman's rank correlation coefficient was used for qualitative variables in ordinal scale (*TUB*, *RIB* and *ECO*), while Pearson's correlation coefficient was applied to quantitative variables. Given that all variables could not be measured for all specimens, correlations used numbers of specimens from between 407 and 524 (450 in most cases).

Distribution of phragmocone size and shape descriptors

Phragmocone diameter distribution at the level of the suture analyzed (Fig. 5, Table 1) is congruent with the results obtained by Raup (1967), who showed that the diameter of most adult, planispiral ammonoids lies between < 20 and 320 mm, with a mean value of ~80 mm. Similarly, Chamberlain & Westermann (1976) recognized a size range of < 10 and 1000 mm, with

Table 1. Upper part: statistics for the analyzed variables. Lower part: Pearson correlations between variables (lower semi-matrix) and statistical level of significance (p) (upper semi-matrix). Correlations for *TUB*, *RIB* and *ECO* were obtained using Spearman's rank coefficient. K: logarithm of the standardized perimeter of sutures. X_c: logarithm of the transitional point between small and large scales of measurement. D_{f1} and D_{f2}: fractal dimensions for both scales of measurement. S_h: sutural height. S_a: sutural amplitude. W: whorl expansion rate. D: distance from the centre of the generating curve to coiling axis. WD: degree of involution. H_2, H_3, H_4, and H_5: amplitudes of the second, third, fourth, and fifth harmonics. P_2 and P_4: phase angles for second and fourth harmonics. H_{4r}: relative amplitude of the fourth harmonic. S: whorl shape. C_2: coefficient of circularity. P_{dia}: phragmocone diameter. W_h: whorl height. *RIB* and *TUB*: relative size of ribs and tubercles, respectively. *ECO*: palaeoenvironment and related paleoecology.

	Sutures						Coiling			Whorl section									Size		Ornamentation		
Statistics	K	X_c	D_{f1}	D_{f2}	S_h	S_a	W	D	WD	H_2	P_2	H_3	H_4	P_4	H_{4r}	H_5	S	C_2	P_{dia}	W_h	*RIB*	*TUB*	*ECO*
N	524	524	524	524	524	524	512	512	512	493	493	493	493	493	493	493	493	493	460	444	527	527	526
Minimum	5.176	1.339	1.060	1.213	12.088	23.077	1.178	0.032	0.070	0.001	90.009	0.001	0.001	45.002	0.005	0	0.345	0.542	6	2.571	1	1	1
Maximum	7.476	1.876	1.462	1.824	69.421	88.095	3.320	0.635	1.090	0.537	179.742	0.140	0.194	89.993	0.653	0.096	1.850	0.963	298	126.273	3	3	3
Mean	6.353	1.548	1.262	1.506	29.635	47.094	2.114	0.339	0.679	0.155	109.315	0.040	0.030	62.399	0.151	0.019	0.890	0.876	61.156	22.656	1.873	1.609	1.517
SD	0.431	0.080	0.074	0.116	8.369	10.645	0.379	0.135	0.224	0.128	32.408	0.024	0.028	18.455	0.115	0.017	0.272	0.065	38.859	13.825	0.751	0.912	0.667
Skewness	0.033	0.568	−0.069	0.097	0.926	0.730	0.733	−0.351	−0.668	0.741	1.427	0.484	2.833	0.535	1.586	1.649	0.399	−1.713	1.318	1.783	0.212	0.849	0.922
Kurtosis	−0.451	0.723	−0.225	−0.431	1.377	0.855	0.009	−0.711	−0.350	−0.427	0.209	−0.174	10.692	−1.559	3.375	2.978	0.054	3.806	3.510	8.209	−1.201	−1.255	−0.318
CV	0.068	0.052	0.058	0.077	0.282	0.226	0.180	0.398	0.329	0.826	0.297	0.598	0.922	0.296	0.757	0.884	0.306	0.075	0.635	0.610	0.401	0.567	0.439
Correlations	K	X_c	D_{f1}	D_{f2}	S_h	S_a	W	D	WD	H_2	P_2	H_3	H_4	P_4	H_{4r}	H_5	S	C_2	$\mathrm{Log_e}(P_{dia})$	$\mathrm{Log_e}(W_h)$	*RIB*	*TUB*	*ECO*
K		<0.001	<0.0001	<0.0001	<0.0001	<0.0001	0.429	0.581	0.419	0.377	0.775	0.469	0.002	0.184	0.098	0.514	0.158	0.884	<0.0001	<0.0001	0.006	0.001	0.004
X_c	−0.167		<0.0001	0.573	0.645	0.428	0.015	0.001	0.001	0.048	0.148	0.007	0.394	0.053	0.537	0.303	0.059	0.125	<0.0001	<0.0001	0.072	<0.001	0.132
D_{f1}	0.812	−0.560		<0.0001	<0.0001	<0.0001	0.807	0.676	0.178	0.276	0.854	0.368	0.004	0.663	0.552	0.402	0.319	0.406	<0.0001	<0.0001	0.821	0.958	0.019
D_{f2}	0.902	−0.025	0.776		<0.0001	<0.0001	0.015	<0.0001	<0.0001	<0.001	0.277	0.409	<0.0001	0.230	0.350	0.061	<0.001	0.003	<0.0001	<0.0001	0.768	0.011	0.003
S_h	0.605	0.020	0.248	0.353		<0.0001	<0.0001	<0.0001	<0.0001	<0.0001	0.024	0.082	0.048	<0.0001	0.001	<0.0001	<0.0001	<0.0001	<0.0001	<0.0001	<0.0001	0.017	0.861
S_a	0.687	0.035	0.317	0.443	0.900		<0.0001	<0.0001	<0.0001	0.001	0.149	0.090	0.276	<0.0001	0.003	<0.0001	0.012	<0.0001	<0.0001	<0.0001	0.002	0.817	0.832
W	−0.036	0.109	−0.011	0.109	−0.277	−0.251		<0.0001	<0.0001	<0.0001	0.009	0.434	<0.0001	<0.0001	0.001	<0.0001	<0.0001	<0.0001	<0.0001	0.005	<0.0001	<0.001	0.908
D	0.025	−0.147	−0.019	−0.172	0.362	0.313	−0.714		<0.0001	<0.0001	<0.001	0.041	<0.0001	<0.0001	<0.0001	<0.0001	<0.0001	<0.0001	<0.0001	0.161	<0.0001	<0.0001	0.759
WD	−0.036	−0.151	−0.061	−0.215	0.297	0.246	−0.435	0.920		<0.0001	<0.0001	0.017	<0.0001	<0.0001	<0.0001	<0.0001	<0.0001	<0.0001	<0.0001	0.923	<0.0001	0.002	0.066
H_2	0.040	0.090	0.050	0.161	−0.211	−0.153	0.417	−0.513	−0.491		<0.0001	0.039	<0.0001	<0.0001	<0.0001	<0.0001	<0.0001	<0.0001	<0.0001	0.017	0.756	<0.0001	<0.001
P_2	−0.013	−0.067	0.009	−0.050	0.103	0.066	−0.122	0.178	0.194	−0.434		<0.0001	<0.0001	0.045	<0.0001	0.001	<0.0001	<0.0001	<0.001	0.014	0.977	<0.0001	0.028
H_3	−0.033	−0.122	0.041	−0.038	−0.079	−0.077	−0.036	−0.094	−0.109	0.093	−0.216		0.387	0.162	<0.0001	<0.0001	0.001	<0.0001	<0.0001	<0.0001	0.756	0.820	0.947
H_4	0.139	0.039	0.131	0.239	−0.090	−0.050	0.294	−0.365	−0.375	0.539	−0.183	0.039		<0.0001	<0.0001	<0.0001	<0.0001	<0.0001	0.574	0.055	0.784	0.954	0.762
P_4	−0.062	0.090	−0.020	0.056	−0.246	−0.219	0.340	−0.461	−0.448	0.757	−0.091	0.064	0.341		<0.0001	<0.0001	<0.0001	<0.0001	<0.0001	0.029	0.973	0.001	0.005
H_{4r}	0.075	−0.028	0.027	0.043	0.147	0.134	−0.155	0.235	0.209	−0.444	0.226	−0.272	0.330	−0.407		<0.0001	<0.0001	<0.0001	<0.001	0.013	0.056	<0.0001	0.002
H_5	−0.030	0.047	0.038	0.086	−0.252	−0.223	0.319	−0.440	−0.430	0.713	−0.157	0.411	0.474	0.624	−0.299		<0.0001	<0.0001	0.049	0.380	0.798	0.018	0.005
S	−0.065	−0.086	−0.046	−0.160	0.179	0.115	−0.364	0.443	0.427	−0.804	0.738	−0.155	−0.409	−0.445	0.319	−0.500		<0.0001	<0.0001	0.032	0.089	<0.0001	0.001
C_2	0.007	−0.070	−0.038	−0.138	0.254	0.216	−0.384	0.527	0.521	−0.862	0.296	−0.212	−0.718	−0.664	0.227	−0.760	0.632		0.001	0.989	0.813	0.008	0.008
$\mathrm{Log_e}(P_{dia})$	0.432	−0.458	0.539	0.330	0.314	0.324	−0.363	0.368	0.261	−0.266	0.177	0.221	−0.027	−0.226	0.186	−0.095	0.234	0.163		<0.0001	0.004	0.028	0.007
$\mathrm{Log_e}(W_h)$	0.471	−0.436	0.587	0.413	0.244	0.262	−0.135	0.067	−0.005	−0.116	0.121	0.288	0.094	−0.108	0.121	0.043	0.104	−0.001	0.950		0.947	0.001	0.002
RIB	0.111	0.064	0.021	0.028	0.184	0.185	−0.325	0.363	0.234	−0.032	0.003	0.030	0.026	−0.003	0.071	0.025	0.061	0.023	0.124	−0.006		<0.0001	<0.0001
TUB	−0.145	−0.170	−0.005	−0.100	−0.082	−0.116	0.164	−0.194	−0.127	−0.272	0.319	−0.042	0.005	−0.154	0.195	−0.094	0.333	0.109	0.088	0.160	−0.401		<0.0001
ECO	−0.119	−0.050	−0.091	−0.122	−0.010	−0.065	0.010	0.032	0.067	−0.166	0.086	−0.006	0.033	−0.118	0.134	−0.117	0.138	0.110	0.115	0.143	−0.353	0.361	

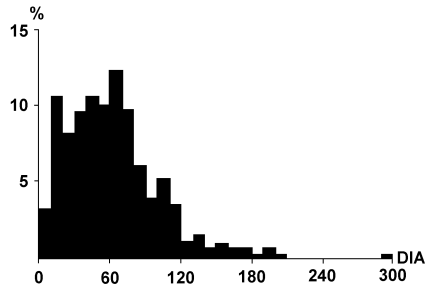

Fig. 5. Frequency distribution of shell diameters in millimetres for the sample of Late Jurassic ammonites.

an average of ~86 mm. Both distributions are right-skewed, as seen in Figure 5. However, the mean value obtained here (61.1 mm) is slightly lower than the latter ones, probably due to our use of phragmocone diameter at the level of the suture analyzed, and not of the maximum diameter of individuals.

Analogously, the distribution of phragmocones in the morphospace defined by parameters *W*, *D* and *S* (Fig. 6A, B) is similar to that of Raup (1967) for the whole set of planispiral ammonites and, in general, corresponds to those obtained by other researchers (e.g. Ward 1980; Saunders & Swan 1984; Saunders & Work 1996, 1997; Dommergues *et al.* 1996). Other values of means and ranges for *W*, *D* and *S* in samples of varying ages are shown in Table 2. Although limits in morphological variation for planispiral phragmocones tend to be constant over geological time, more densely occupied regions of the morphospace may vary among periods. The distribution of the phragmocones we analyzed coincides with results obtained by Ward (1980) for the Jurassic and by Dommergues *et al.* (1996) for the Early Jurassic, a time interval in which shells commonly show low *W*, high *D*, and intermediate *S* (~1) values. Our sample of Late Jurassic ammonites shows a higher density of evolute shapes with circular whorl sections than the one analyzed by Bayer & McGhee (1984) for the Middle Jurassic. Given these results, size and shape distributions obtained for Late Jurassic phragmocones may be considered representative of ammonites and show no significant bias that could otherwise invalidate our inferences.

As regards to other morphometric descriptors used to characterize whorl section, the inverse relationship between harmonic amplitudes and the circularity coefficient C_2 is worthy of note (Table 1). This was expected since these variables indicate the degree to which a circle must be deformed in order to fit whorl section shapes. It should be kept in mind that depressed whorl sections, although elongated, generally display more circular outlines than compressed ones. As can be seen in Figure 6C, distribution of C_2 values in the vicinity of $S = 1$ is not symmetrical.

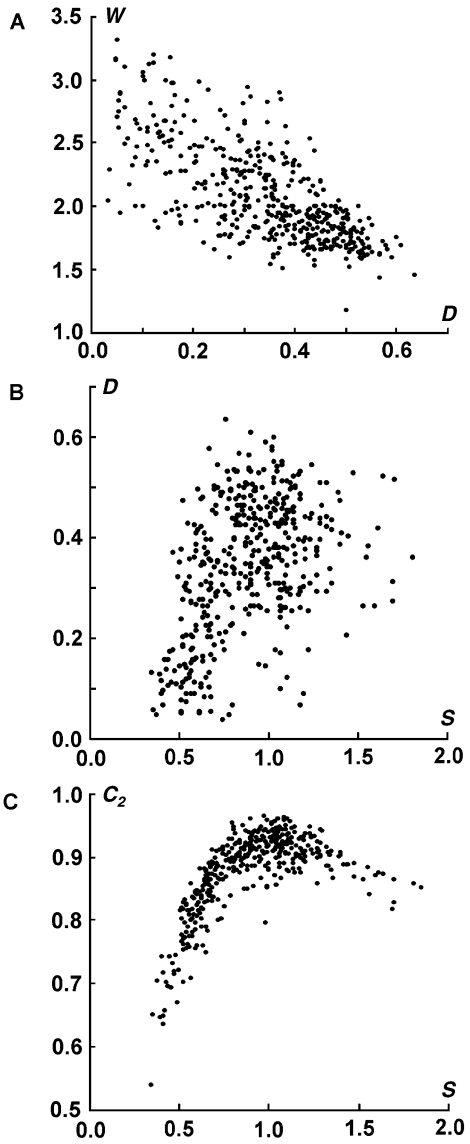

Fig. 6. Bivariate plots of Raupian parameters (*W*, *D*, *S*) and circularity index (C_2) for the specimens analyzed in this study.

The most relevant geometric whorl section components can be characterized with a relatively low number of harmonics, given the results obtained in a principal components analysis in which the amplitudes of harmonics 2–5 are used as variables. Figure 7 shows whorl section scores on the first two components, which jointly account for 85% of the original variance, and the position of several sections, which reveals that these components depict a smooth morphological gradient. Given the factor loadings of variables on both axes, the first component describes whorl-section elongation since the most compressed outlines take positive projections on this axis, whereas quadrangular and circular sections tend to score on its negative values. The second component reveals

Table 2. Mean and range of values of whorl expansion rate (*W*), distance to coiling axis (*D*) and whorl shape (*S*) for planispiral ammonoids in different geological periods.

		W			*D*			*S*			
Age	*N*	Min.	Max.	Mean	Min.	Max.	Mean	Min.	Max.	Mean	References
Devonian	205	1.13	5.01	2.17	0.00	0.75	0.27	0.33	3.21	0.87	Saunders *et al.* (1999, 2004)
Lower-Middle Carboniferous (Namurian)	531	1.19	3.40	1.97	0	0.57	0.24	0.38	3.17	1.35	Saunders & Swan (1984)
Middle-Upper Carboniferous (Pennsylvanian)	117	1.20	3.20	1.90	0.02	0.59	0.24	0.33	2.82	1.26	Saunders & Work (1996)
Carboniferous	255	1.20	4.00	1.91	0.00	0.60	0.22	0.23	2.82	1.20	Saunders *et al.* (1999, 2004)
Permian	148	1.20	3.64	1.99	0.00	0.69	0.20	0.29	2.86	1.15	Saunders *et al.* (1999, 2004)
Middle Devonian to Upper Permian	53	1.40	3.15	1.95	0	0.89	0.21	0.41	2.76	1.28	Saunders (1995)
Early Triassic	11	1.57	2.45	2.05	0.15	0.55	0.33	0.46	1.97	0.83	Saunders *et al.* (1999, 2004)
Triassic	322	1.20	4.34	–	0.00	0.60	–	0.21	2.42	–	McGowan (2004)
Lower Jurassic	436	~1.38	~4.3	–	~0.02	~0.78	–	~0.2	~2.2	–	Dommergues *et al.* (1996)
Middle Jurassic	507	1.50	3.00	2.10	0.03	0.49	0.24	~0.33	~1.1	0.54	Bayer & McGhee (1984)
Upper Jurassic	511	1.18	3.32	2.11	0.03	0.64	0.34	0.35	1.85	0.89	This article
Jurassic	587	~1.30	~2.9	–	~0.03	~0.70	–	~0.3	~1.6	–	Ward (1980)
Cretaceous	292	~1.39	~3.3	–	~0.01	~0.53	–	~0.3	~1.75	–	Ward (1980)
Jurassic to Cretaceous	71	1.46	3.58	2.27	0.04	0.53	0.27	0.29	1.39	0.80	Almeida *et al.* (1974)
Palaeozoic to Mesozoic	405	~1.14	~3.28	2.13	~0	~0.67	0.29	~0.2	~1.4	0.82	Raup (1967)

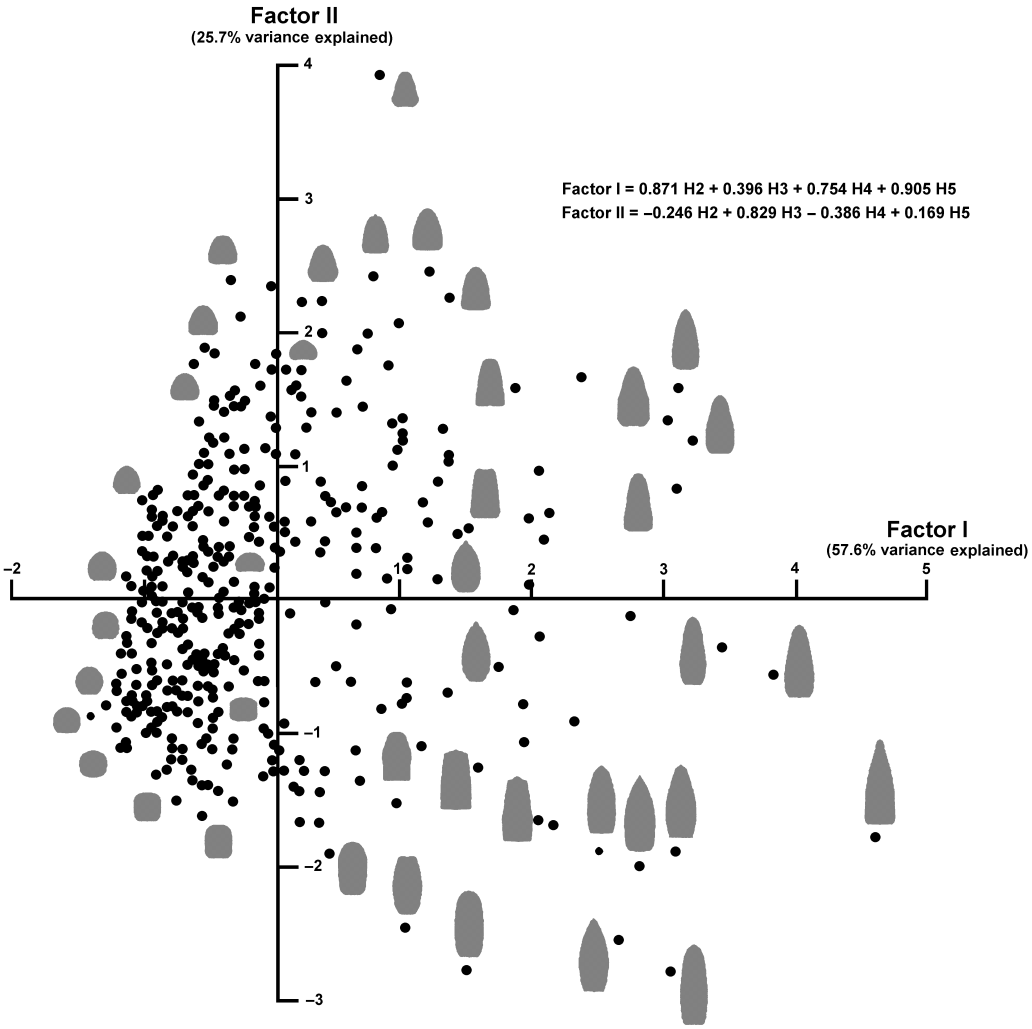

Fig. 7. Bivariate scatter plot of factor scores for the specimens analyzed on the first two factors obtained using the first five harmonic amplitudes as variables. Examples of the projections of selected whorl sections are shown.

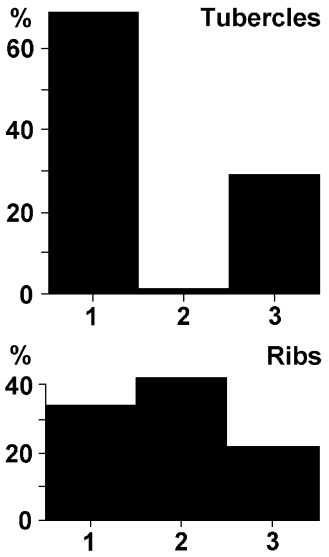

Fig. 8. Frequency distributions for occurrence and size of tubercles and ribs in the sample of Late Jurassic ammonites (1: without ornamental elements; 2: small- to medium-sized elements; 3: large elements).

the degree of whorl-section triangularity since trapezoidal sections occupy an intermediate position between rectangular and triangular ones. Depressed sections score close to zero on the first component, while on the second axis they are projected in accordance with their degree of triangularity. Thus, they are placed between the morphospace regions for compressed sections and for both circular and squared sections, although closer to the latter two. This is due to the fact that depressed whorl sections, although somewhat elongated, are more rounded than compressed ones. Finally, pentagonal sections, which also tend to be elongated, are placed closer to triangular sections than to quadrangular ones.

Concerning ornamental features, Figure 8 shows that: (1) ribbed phragmocones are more common than those without ribs; (2) the most abundant phragmocones are those with small- to medium-sized ribs; (3) phragmocones with tubercles are less common than those without them; and (4) phragmocones with large-sized tubercles are more frequently found than those with small ones, which only represent 2% of the dataset.

Table 1 shows that correlation values for morphometric variables characterizing size, shape and ornamental features in phragmocones are low, although some of them are significant and evidence of interesting relationships. There is, for example, an inverse relationship between the development of tubercles and ribs ($r_{TUB\text{-}RIB} = -0.40$, $P < 0.00001$). Both of these variables are diversely related to whorl coiling: in phragmocones, tubercle development appears to covary with the degree of involution ($r_{TUB\text{-}WD} = -0.13$, $P = 0.002$) and whorl compression ($r_{TUB\text{-}S} = 0.33$, $P < 0.0001$), whereas ribs tend to be larger and more abundant when coiling is looser ($r_{RIB\text{-}WD} = 0.23$, $P < 0.0001$). In addition, no significant relationship was found between ribs and morphometric whorl section descriptors. Several authors (e.g. Buckman 1892; Westermann 1966, 1971; Raup 1967; Cowen *et al.* 1973; Bayer & McGhee 1984; Guex *et al.* 2003) have examined the covariation in ornamentation and shell morphology in ammonoids, concluding that a direct relationship exists among ornamentation degree, umbilicus openness, and whorl section circularity (what Westermann (1966) called the 'First Buckman Law of Covariation'). Results obtained by Yacobucci (2004) suggest that this 'law' is not universal, since it does not appear to be valid for some Cretaceous acanthoceratids, but it is worth noting that Buckman (1892) defined it in terms of intraspecific variation (see Hammer & Bucher 2005). This study partially corroborates such a relationship or 'law' in ornamented shells: rib and tubercle size increase with phragmocone diameter regardless of whorl height, which reveals the greater development of these ornamental elements in evolute phragmocones. However, it is worth noting that the correlations obtained are remarkably low, particularly in the case of tubercles (Table 1). This reinforces the notion that different ornamental features must be considered independently, since constraining constructional, phylogenetic and/or functional factors may impose on such ornamental features an imbalanced influence. In any case, covariation among size, morphology and ornamentation is remarkably weak, and nearly any combination of such features can be found. Thus, the results obtained must be considered with caution until more detailed analyses conducted under phylogenetic control are available.

In addition, the weak relationship between the palaeoenvironment and related palaeoecology and phragmocone size and shape must be stressed. Our results evidence only subtle trends, as in the case of ornamental features. Epioceanic ammonites usually show more circular whorl sections than neritics ($r_{ECO\text{-}H2} = -0.17$, $P < 0.001$), independently of whorl coiling, though this could be partially due to taphonomic noise. However, as we discuss in depth below, the most interesting result is potentially the positive correlation between the record of epioceanic ammonites, and both phragmocone size and whorl height (see Table 1).

Distribution of sutural descriptors

Figure 9 shows histograms for variables related to sutural complexity (see also Table 1). Normal distri-

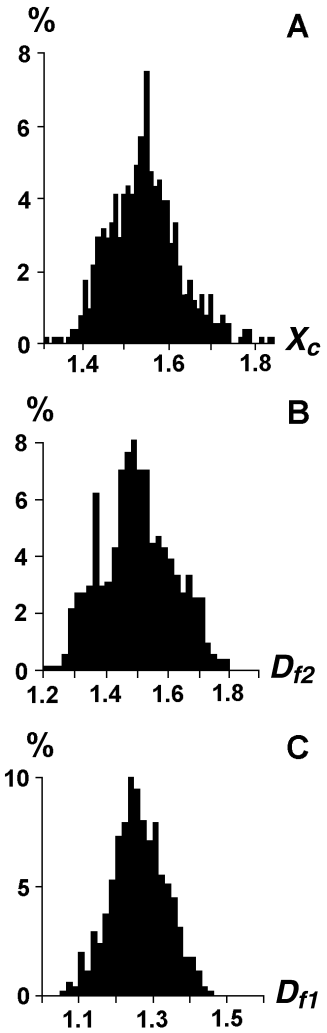

Fig. 9. Frequency distributions for (A) the inverse self-similarity index (X_c) and fractal dimensions at (B) large (D_{f2}) and (C) small (D_{f1}) scales of measurement.

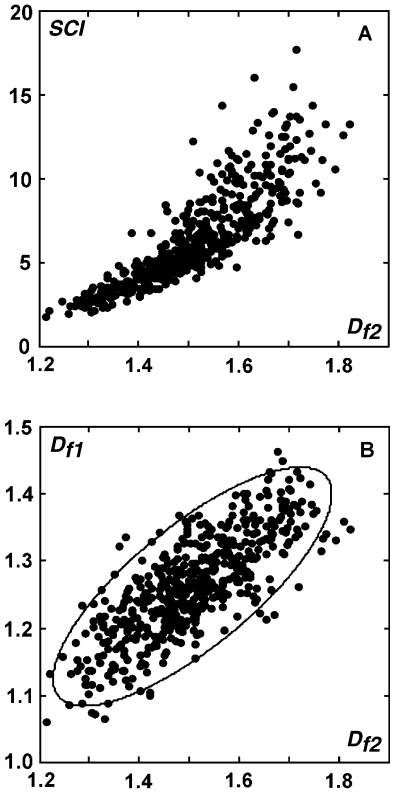

Fig. 10. Bivariate scatter plots showing the behaviour of some of the sutural variables analyzed: □A. index of sutural complexity (*SCI*) vs. fractal dimension at large scales of measurement (D_{f2}), □B. the fractal dimension values for both scales of measurement (D_{f1} vs. D_{f2}). The ellipse in (B) represents the 95% confidence region of the plot.

bution for these variables was evaluated using the Kolmogorov–Smirnoff test.

When a power function is fitted to the bilogarithmic plot of sutural perimeter (*y*-axis) on ruler size (*x*-axis), the mean for X_c (1.548, Fig. 9A) shows significant difference ($P < 0.001$) from the theoretical value expected, 1.275. Hence, the ammonitic sutures analyzed start to lose their fractal character at the scale of measurement $e^{1.548}$, which corresponds to 4.7% of the length of a line connecting the ends of both sutures. The values observed for this lower limit of self-similarity range between 3.8% and 6.5%, which agrees with the results obtained by Lutz & Boyajian (1995). These authors found a range of 1.5% to 12%, in which the highest frequencies were between 1.5% and 6%. This is interesting since Lutz & Boyajian (1995) visually estimated the lower limit of self-similarity and their sample included not only ammonitic, but also goniatitic and ceratitic sutures.

Distributions of D_{f2} and D_{f1} values (Figs. 9B, C) have a certain degree of symmetry, with non-significant deviations from normality, although the fractal dimension at large scales shows a relative maximum at approximately 1.35 (Fig. 9B). Table 1 shows that the mean of D_{f2} is close to 1.5. This suggests a degree of complexity halfway between a straight line ($D = 1$) and an intricate curve that would fill a plane ($D = 2$) in the sutures analyzed. The value 1.5 is similar to that obtained by Lutz & Boyajian (1995) for D_f in ammonitic sutures (1.46), as well as their range of values (1.21–1.71) with respect to our estimate (1.21–1.82).

Figure 10A shows a direct relationship between the index of sutural complexity (*SCI*) and D_{f2}. This also agrees with results in Lutz & Boyajian (1995), although the exponential behaviour of *SCI* induces higher point-dispersal when fractal dimension values increase. The sutures that more closely fill a plane do not thus necessarily show a longer normalized perimeter. In addition, Figure 10A reveals a greater scatter of *SCI* at high D_{f2} values, which reflects decoupling of *SCI* at high (D_{f2}) and low (D_{f1}) scales of measurement.

The absence of correlation between D_{f2} and X_c is analogous to that obtained by Lutz & Boyajian (1995) for ammonoids as a whole. However, the strong and statistically high-significant negative correlation between X_c and D_{f1} ($r_{XC\text{-}Df1} = -0.56$, $P < 0.0001$) suggests that the more pervasive the folding of smaller portions of the suture, the lower the loss of its fractal nature. Differential behaviour of D_{f1} and D_{f2} with X_c is, in any case, of particular relevance, given that the correlation between both fractal dimensions is very high ($r_{Df1\text{-}Df2} = 0.78$, $P < 0.0001$; Fig. 10B, Table 1). In addition, correlations of D_{f2} and X_c with the difference between D_{f2} and D_{f1} in relation to the value of D_{f2} (i.e. $D_f = (D_{f2} - D_{f1})/D_{f2}$) are positive ($r_{Df\text{-}Df2} = 0.65$; $r_{Df\text{-}Xc} = 0.64$; $P < 0.0001$ in both cases). This indicates that more complex sutures show a greater difference of complexity between both scales of measurement and that such a difference is linked to an early loss of self-similarity. In fact, there is a high positive correlation between D_{f2} and X_c where D_f remains constant ($r_{Xc\text{-}Df2.Df} = 0.76$; $P < 0.0001$). These results suggest that complexity loss at smaller scales of observation is biased, since the most complex suture lines display a greater difference between the synthesized suture perimeter and the perimeter they would theoretically reach if they behaved as a pure, mathematical fractal '*ad infinitum*'.

Phragmocone size and sutural complexity

The covariation between sutural complexity and phragmocone size is one of the most relevant contributions of this study. In general, phragmocone size increase implies more complex sutures in ammonites, this resulting from subdivision and corrugation of lobes and/or saddles, as well as from the addition of new sutural elements. Although the ontogenetic complication of septal sutures varies among groups, major sutural features (e.g. number, position and relative size of major lobes) vary less at higher taxonomical levels, hence their taxonomical value (see Kullmann & Wiedmann 1970).

Major changes in sutural complexity take place at early ontogenetic stages (Lutz & Boyajian 1995) and mean sutural complexity increases progressively, slowing down over the remaining ontogeny (Arkell *et al.* 1957; García-Ruiz *et al.* 1990; Saunders & Work 1997), although there are examples of ontogenetic sequences with sutures that show a slight decrease in complexity (García-Ruiz *et al.* 1990). Only adult specimens were selected for this study in order to minimize ontogenetic variability – a common practice when sutural complexity is compared across taxonomic categories above the species level. It is worth mentioning, however, that the main source of variation in phragmocone size and sutural design arises from phylogeny.

Table 1 shows that the most significant correlations involving sutural parameters (except correlations among themselves) apply to variables that reflect phragmocone size. Among them are several direct and statistically highly significant correlations between fractal dimensions and the logarithms of phragmocone diameter and, specially, whorl height (Fig. 11A–D, Table 1). Given that whorl height and phragmocone diameter correlate well in the sample, we performed a *t*-test evaluation of differential values between correlation coefficients of fractal dimensions with whorl height and phragmocone diameter (i.e. H_o: $r_{Df\text{-}Wh} = r_{Df\text{-}Pdia}$). This revealed a significant difference of correlation coefficients for D_{f2}-W_h and D_{f2}-P_{dia} ($t = 5.48$, $P < 0.001$) as well as for D_{f1}-W_h and D_{f1}-P_{dia} ($t = 3.83$, $P < 0.001$).

Coefficients of partial correlation for sutural complexity at small and large scales of measurement with whorl height, assuming that phragmocone diameter is held constant and vice versa, were estimated on these grounds. Partial correlation of D_{f1} with $\log_e(W_h)$ is highly significant ($r_{Df1\text{-}Log(Wh).log(Pdia)} = 0.29$, $t = 5.84$, $P < 0.0005$), while partial correlation of D_{f1} with $\log_e(P_{dia})$ does not differ from zero ($r_{Df1\text{-}log(Pdia).log(Wh)} = -0.09$, $t = -1.74$, $P > 0.05$). D_{f2} shows a similar behaviour with respect to W_h ($r_{Df2\text{-}Log(Wh).log(Pdia)} = 0.33$, $t = 6.63$, $P < 0.0005$), although the partial correlation with $\log_e(P_{dia})$ is negative ($r_{Df2\text{-}log(Pdia).log(Wh)} = -0.21$, $t = -4.22$, $P < 0.0005$). Positive correlation between D_{f1} and P_{dia}, in addition to the absence of correlation when W_h is constant, confirms that W_h is more appropriate than P_{dia} for these studies (as envisaged by Newell 1949). Negative partial correlation of D_{f2} and P_{dia} arises from the low but significant correlation between sutural complexity and phragmocone shape: the most involute phragmocones (i.e. those with a higher W_h:P_{dia} ratio) show more complex sutures for a given whorl height. Furthermore, the absence of significant differences ($t = 0.55$; d.f. = 381; $P > 0.7$) between correlation coefficients of X_c with $\log_e(W_h)$ and $\log_e(P_{dia})$ determines the low resolution of these partial correlations, thus confirming weak and inverse relationships of X_c with both W_h and P_{dia} (see Table 1 and Fig. 12A, B).

The relationship between X_c and phragmocone size can be clarified by analyzing this parameter of sutural complexity at real scale (X_{cr}), that is, for sutures at actual scale in millimetres. X_{cr} was estimated assuming a correspondence between the length of a straight line joining the suture ends and the perimeter of the flank. Figure 12C, D shows values of X_{cr} in relation to $\log_e(P_{dia})$ and $\log_e(W_h)$, respectively. Correlations of X_{cr} with both variables are 0.98 and

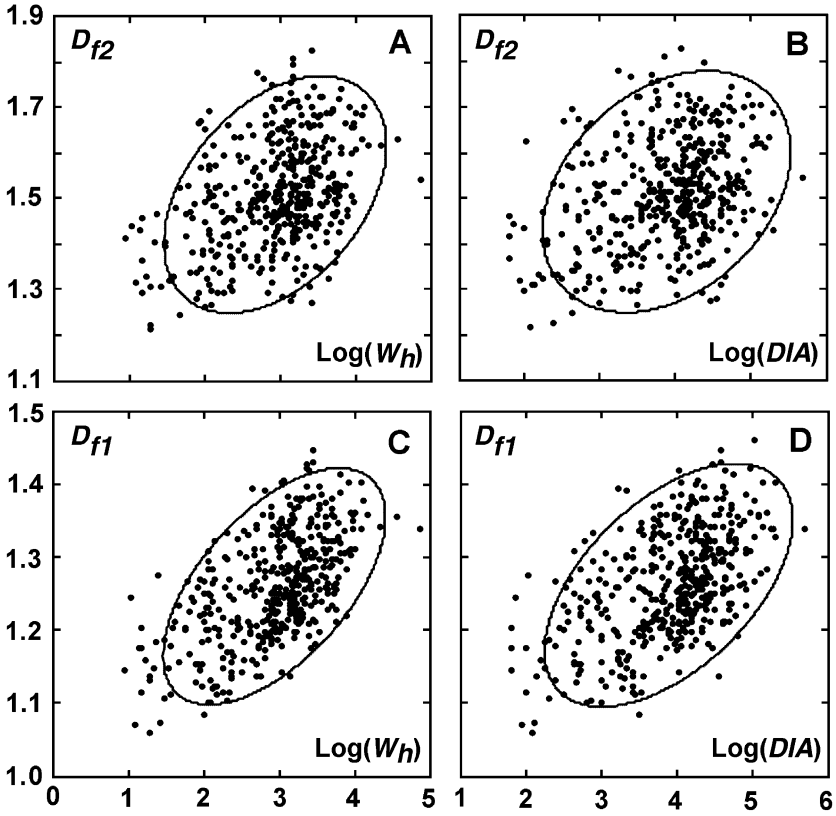

Fig. 11. Bivariate scatter plots for both fractal dimensions (D_{f1}, D_{f2}) vs. the logarithms of whorl height (A, C) and phragmocone diameter (B, D) The ellipses represent the 95% confidence regions of these plots.

0.95 ($P < 0.0001$ in both cases), respectively. This indicates that the self-similarity of sutures reaches smaller regions in the smallest flanks, whereas sutures in flanks belonging to the highest whorl sections show a self-similar nature within a narrower range of scales of measurement. Thus, the largest phragmocones have minor lobes and saddles of greater size than do smaller phragmocones. However, this is obscured when the sutures are standardized to a length of 100 arbitrary units. In this case, the lower limit of self-similarity (X_c) correlates negatively with whorl height and phragmocone diameter (Fig. 12A, B, Table 1). This is because the less self-similar sutures are those of smaller length.

Comparison of differences between correlation coefficients of X_{cr} with W_h and P_{dia}, respectively, makes it possible to reject the null hypothesis of equality between them ($t = 10.41$, $P < 0.0005$). On this basis, it was appropriate to analyze the partial correlations of X_{cr} with $\log_e(P_{dia})$ and $\log_e(W_h)$. The value for $r_{Xcr\text{-}log(Wh).log(Pdia)}$ is 0.80 ($t = 26.12$, $P < 0.0001$) and for $r_{Xcr\text{-}log(Pdia).log(Wh)}$ decreases to 0.27 ($t = 5.54$, $P < 0.0001$). These results confirm that the point below which suture self-similarity no longer holds is mainly determined by whorl height and secondarily by phragmocone diameter (i.e. at last by the degree of coiling and whorl overlapping).

In summary, all of the ammonites analyzed display positive correlations between fractal complexity, in a wider sense, and whorl height, while no regular, uniform correlations were found with phragmocone diameter and the possibility of negative correlations should not be discarded. This suggests that, for a given whorl height, the most evolute phragmocones (i.e. those with a lower W_h:P_{dia} ratio) must develop a higher number of whorls than the most involute ones before acquiring similar levels of sutural complexity. In addition, the size of minor lobulations in the highest flanks is also greater than in smaller ones, although the sutures in the former show higher levels of self-similarity.

Phragmocone shape and sutural complexity

The relationship between sutural variables and phragmocone shape is more complex than for phragmocone size, and additional morphometric descriptors must be considered.

Absolute correlations between variables describing sutural traits and those related to phragmocone shape

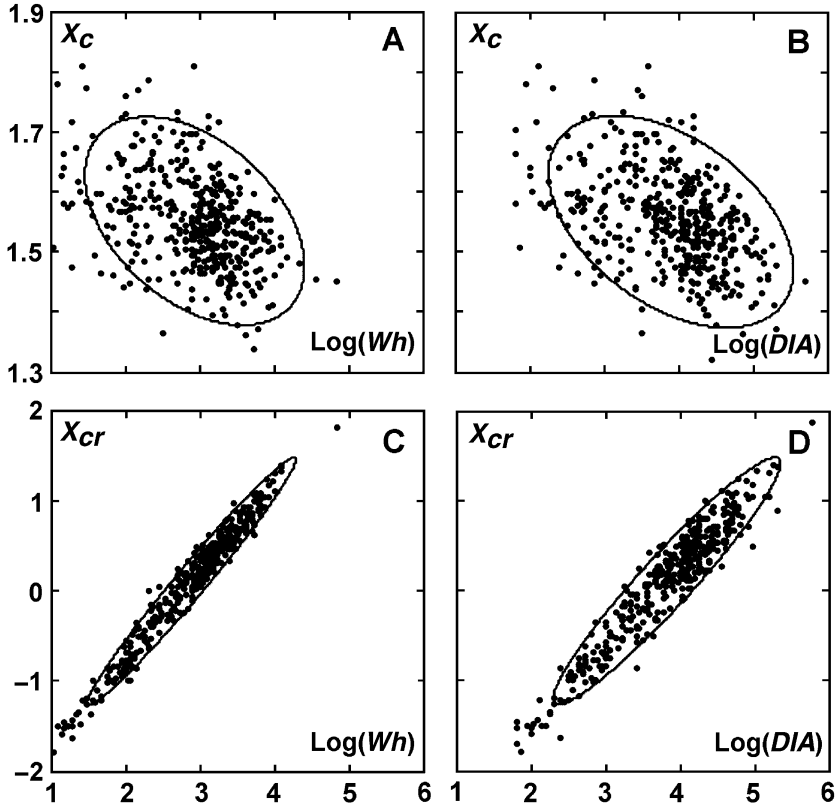

Fig. 12. Bivariate scatter plots for the inverse self-similarity index of sutures (X_c: logarithm of the scale of measurement for standardized sutures below which their self-similar character disappears; X_{cr}: the same for sutures at actual scale, in mm) vs. the logarithms of whorl height (A, C) and phragmocone diameter (B, D). The ellipses represent the 95% confidence regions of these plots.

(Table 1) display some differences with the ones previously discussed for phragmocone size – e.g. correlations for shape variables are clearly much lower. In addition, for the most part the only sutural variables that show significant correlations with phragmocone and whorl shape are those related to suture geometry at large scales of measurement.

Where W_h is constant (Table 3), a set of significant correlations can be observed between sutural variables and phragmocone shape descriptors, although there are some exceptions for X_c and K. Independent relationships therefore exist between phragmocone size and both sutural and shape features, as revealed by the comparatively lower correlations between flank height and the morphological variables of phragmocones. Furthermore, almost all pairs of variables display inhibitory effects on the covariance between sutural variables and morphometric descriptors of whorl shape. This is evidenced by the increased value of partial against absolute correlations (compare values in Tables 1, 3).

Correlation between variables characterizing coiling and fractal dimension for large scales of measurement (Table 3) shows that the latter increases as coiling becomes tighter (positive correlation of D_{f2} with W and negative one with D). This is even more evident with respect to WD, since its correlation with D_{f2} (–0.24) is slightly more significant than in the case of W (0.20) and D (–0.23).

Correlations between morphometric descriptors of whorl shape and fractal dimension at large scales of measurement are significant for the amplitudes of the second and fourth harmonics but not for the amplitude of the third harmonic (Table 1, lower part: upper semi-matrix). These correlations are also higher when phragmocone size effects are removed, even though the values continue to be low. In addition, it is worth noting that there is a significant negative correlation between D_{f2} and H_3 if whorl height is held constant (Table 3).

Correlations between fractal dimension and H_2, S and C_2, respectively, indicate that D_{f2} increases with whorl section elongation (i.e. circularity loss) and with the degree of polygonality, which is not, however, strictly related to whorl elongation. Interrelationships among D_{f2} and H_2, S and C_2 are evidenced by their partial correlations (Table 3), which show the same value of variance and null coefficients, although the absolute coefficients are significantly distinct from zero, since S and C_2 are inversely

Table 3. Values and statistical significance of partial correlation coefficients between sutural variables and morphometric descriptors of phragmocones, calculated by keeping whorl height (W_h) constant.

	W	D	WD	H_2	H_3	H_4	H_{4r}	H_5	S	C_2	P_2	P_4
K	0.083**	− 0.065*	− 0.082**	0.137***	− 0.188****	0.158****	0.021*	− 0.031*	− 0.137***	− 0.049*	− 0.080*	0.040*
X_c	0.053*	− 0.133***	− 0.167****	0.083**	− 0.051*	0.125***	0.045*	0.086**	− 0.077*	− 0.119***	− 0.022*	0.071*
D_{fl}	0.108**	− 0.088**	− 0.081**	0.171****	− 0.146***	0.125***	− 0.063*	0.027*	− 0.149***	− 0.079*	− 0.094**	0.087**
D_{f2}	0.200****	− 0.234****	− 0.240****	0.272****	− 0.193****	0.278****	0.012*	0.095**	− 0.248****	− 0.210****	− 0.128***	0.162****
S_a	−0.124***	0.207****	0.180****	− 0.160****	− 0.187****	− 0.034*	0.159****	− 0.196****	0.166****	0.166****	0.105**	− 0.161****

****: $P < 0.001$, ***: $P < 0.01$, **: $P < 0.05$, *: $P > 0.05$.

related to H_2 (−0.80 and −0.86, respectively) and D_{f2} (−0.16 and −0.14, respectively). Partial correlations of C_2 and S with D_{f2} reveal a close relationship between whorl elongation and D_{f2}, indicating that S correlates with D_{f2} through its correlation with C_2. It could thus be assumed that there is no correlation between D_{f2} and the absence of circularity in depressed sections ($S > 1$). However, this feature may be masked given that the degree of circularity is higher in depressed sections than in compressed ones ($S < 1$).

Another point that should be underlined is the positive relationship between the fourth harmonic amplitude and D_{f2}, although whether it depends on a given orientation of H_4 must be clarified. Of particular relevance is the direct and significant partial correlation of D_{f2} with the phase angle of this harmonic (see Table 3). The positive correlation reveals that H_4 shows higher values when positioned around 90° than when nearing 45°, thus contributing to the degree of elongation of laterally compressed whorls. This interpretation is reinforced by the absence of a significant absolute correlation between H_{4r} and D_{f2} (Table 1), given that the value of H_{4r} is important only when the fourth harmonic is oriented around 45°. This implies that section quadrangularity does not *sensu stricto* correlate with sutural complexity.

Concerning relative suture amplitude (S_a), shape descriptors show significant relationships with the same variables as does fractal dimension, but the relationships in this case are inverted. S_a decreases with both phragmocone lateral compression and coiling degree and thus correlates directly with quadrangularity. This implies that S_a and D_{f2} do not share the same variance in their relationships with phragmocone shape, irrespective of their strong correlation, thus displaying the opposite behaviour. On this basis and in reference to whorl-shape related variables, it may be deduced that the generator length for fractal complexity at large scales of measurement ($L_{max2} = e^{n/Df2}$) behaves similarly to S_a but contrasts with D_{f2}. However, unlike S_a, L_{max2} correlates positively with D and inversely with H_2, but not with section quadrangularity.

Finally, X_c, D_{fl} and D_{f2} show significant positive correlations with phragmocone morphometric descriptors, even when the effects W_h are removed. Our sample, however, reveals that the most evolute specimens, which develop markedly circular sections, show larger phragmocone diameters, although flank height is not related to phragmocone shape. Thus, if phragmocone diameter is held constant, partial correlations between phragmocone shape and X_c will not be significant. The relationship between X_c and phragmocone shape variables will then be indirectly determined by the covariance of X_c and phragmocone diameter.

Sutural complexity and type of ornamentation

As shown in Table 1, the relationship between sutural variables and the type and degree of development of ornamental features is very weak, as is also the case for the rest of the morphological variables describing phragmocone shape. However, a slight trend exists towards increasing standardized sutural perimeter K when rib sizes are larger ($r_{K\text{-}RIB} = 0.11$), and a reversed trend in tubercles ($r_{K\text{-}TUB} = -0.15$). Only the latter trend holds for D_{f2}, although the correlation is very weak ($r_{Df2\text{-}TUB} = -0.10$). The most significant relationships of sutural variables concerns S_h ($r_{RIB\text{-}Sh} = 0.18$) and S_a ($r_{RIB\text{-}Sa} = 0.19$), indicating that more strongly ribbed phragmocones also show sutures with greater sutural amplitudes and normalized lobe or saddle heights, although this behaviour tends to be reversed where large tubercles are the most relevant ornamental features. These significant correlations suggest the existence of constructional relationships between septal and ornamental features. However, it should not be forgotten that phylogenetic factors, as well as the indirect covariation between ornamentation and phragmocone morphology, may also be influential.

Sutural complexity and palaeoecology

Table 1 gives values for Spearman's rank-order correlation between palaeoenvironmental variables, sutural variables and those related to phragmocone size and shape. Once again, it is striking that no high correlations appear, although many are significant at $P < 0.05$ or even higher levels of confidence. Also interesting is the lack of significant correlations between palaeoenvironmental and sutural variables, with the exception of the inverse correlations for both scales of measurement and for K, which is proportional to the logarithm of *SCI*. On average, epioceanic specimens thus tend to show lower values in sutural complexity and a less standardized sutural perimeter. As discussed above, sutural complexity and palaeoenvironment positively correlate with phragmocone size. Nevertheless, epioceanic ammonites that do not evidence significant taphonomic noise exhibit larger phragmocone size than neritic ones, although they show less sutural complexity on average.

Discussion

One of the most relevant results obtained in this study is the close relationship between sutural complexity, as measured by both D_f values, and flank size. This result contrasts with the findings of Boyajian & Lutz (1992) and Lutz & Boyajian (1995), who argued that there is no correlation between sutural complexity and shell size in ammonoids. Such a discrepancy is significant, since coherence is complete between our results and the ones obtained by these authors, despite differences between the respective samples; the samples studied by Boyajian & Lutz (1992) and Lutz & Boyajian (1995) are more diverse in timespan, taxonomy and basic sutural types. In fact, no significant relationship is evident between sutural complexity and phragmocone size in a sample that comprises goniatitic, ceratitic and ammonitic sutures. This may distort the perception of such a relationship in a subsample (e.g. the ammonitic sutures studied). Our case-study, which concerns substantial differences in shell shape and/or a narrow size range, precludes the search for the effects of phragmocone diameter on sutural complexity, since fractal dimension correlates more tightly with whorl height than with phragmocone diameter.

Our results suggest that the morphogenetic mechanisms that accounts for septal folding, and thus for complex suture development, would interact with the size of the phragmocone portion in which these structures are placed. This implies that sutural complexity is more closely linked to a 'local phenomenon', which in turn is related to the growth pulse at the level of the most recently formed septum. Any process that takes the absolute dimensions of the ammonite shell directly into account is of minor importance and, in contrast, a physiological process associated with the energetic demands of metabolism has recently been proposed by Pérez-Claros (2005) for interpreting main factors controlling suture complexity. The strong relationship observed here between whorl height – which measures the size of the animal residing in a given whorl – and sutural complexity reinforces this hypothesis.

If no relationship exists between structural shell weakness against hydrostatic load or against any other extrinsic factors and decreasing shell wall strength with phragmocone size, as suggested by Hewitt & Westermann (1997), our results would not allow us to conclude that greater complexity in septal sutures would imply greater resistance. Our results, however, are coherent with the alternative hypothesis according to which sutural complexity was related to other alternative functions, such as buoyancy control through the enhancement of surface tension phenomena (e.g. Kulicki 1979; Ward 1987; Kulicki & Mutvei 1988; Weitschat & Bandel 1991; Saunders 1995; Daniel *et al.* 1997; Kröger 2002). An increase in phragmocone size would thus imply greater volumes of water pumping, a function that would be facilitated by increased lobe and saddle sinuosity. This would lead to a higher number of septal 'receptacles', thus facilitating

capillary phenomena – i.e. chamber emptying and/or occasional refilling. However, it is necessary that such a hypothesis be verified because tensional surface phenomena in this type of interphase are inversely related to the radius of shell-wall curvature. Surface tension could be compensated or even decreased, given that the size of the smaller sinuosities (i.e. those that have a higher pressure potential) is also enlarged with flank size. Further research will be needed in order to clarify the relationships among tensional surface phenomena in septal sutures, their fractal dimension and lobe and saddle size distribution.

The relationship between phragmocone shape and sutural complexity we found in Late Jurassic ammonites is analogous to the one found by Saunders & Work (1997) in prolecanitids, although they quantified sutural complexity using a different procedure. The *SCI* index correlates well with D_f in sutures figured by Saunders & Work (1997). Such a correlation is impressive, since prolecanitids and Late Jurassic ammonites are temporally and phylogenetically distant, and exhibit distinct levels of sutural complexity. This fact, therefore, reinforces the hypothesis that covariation between phragmocone shape and sutural complexity in ammonoids relies more on functional (soft-body) grounds than on constructional (mineralized structures) limitations. The implications of phylogenetic factors should, however, always be kept in mind, given that prolecanitids represent the 'rootstock' of Mesozoic ammonites (Saunders & Work 1997). Moreover, there are groups, such as the goniatitids, in which the relationships we describe between sutural complexity and phragmocone shape are entirely absent (e.g. Saunders & Work 1996).

It is possible that covariation between sutural complexity and phragmocone shape is a consequence of functional demands. An assumed correspondence between potentially deeper habitats for ammonoids and distance-to-shoreline has been traditionally accepted. Recent data, however, disconfirm the hypothesis that greater degrees of septal folding are mainly related to structural resistance against hydrostatic loadings in phragmocones. In fact, our results indicate that Late Jurassic epioceanic ammonites generally show less sutural complexity than neritic ones, in agreement with previously published conclusions (Olóriz & Palmqvist 1995; Olóriz *et al.* 1997, 1999, 2002). Theoretical studies conducted using finite-element analysis (Daniel *et al.* 1997) related increases in septal folding to a weakened septum against hydrostatic load (but see Hassan *et al.* 2002). Despite the fact that epioceanic ammonites usually display phragmocones of larger diameter and whorl height than do epicontinental ones, in our sample they show a slightly lower sutural complexity. If septal folding is mainly related to phragmocone reinforcement, covariation with shell morphology could then satisfy demands other than hydrostatic load – e.g. resistance to predator teeth (Daniel *et al.* 1997). Recently, however, some of the most spectacular examples of 'bite-marks', interpreted as a result of mosasaur attacks, have been questioned (e.g. Olóriz *et al.* 2002). Considering the role played by tensional surface processes, some relationships with buoyancy control are enhanced. Hence, covariation with phragmocone shape could depend on process relationships with the shape of the 'receptacle' containing cameral fluids. Three-dimensional sinuosity of septa leads to closer lobes and saddles in opposite flanks of the most involute phragmocones showing more elongated sections. This would influence surface-strain phenomena, which would be favoured by the existence of organic structures, regardless of whether they are associated with the siphuncle. Such organic structures have been described in Palaeozoic and Mesozoic ammonoids (e.g. Permian prolecanitids in Mapes *et al.* (1999) and Tanabe *et al.* (2000); Triassic ceratitids in Weitschat & Bandel (1991); and Late Jurassic ammonites in Schindewolf (1968)). In addition, an indirect connection between sutural complexity and buoyancy control should not be neglected, given that sutural complexity appears to comply with some of the key rules regarding metabolic or physiological processes (Pérez-Claros 2005). Given that phragmocone chambers were filled with wettable organic tissues produced by the rear mantle, sutural complexity may result from a need for increasing mantle surface area. Such an increase would be a solution, since phragmocone chambers must be built up under spatial constraints defined by the carcass. This solution is not unusual in the animal kingdom (e.g. mammalian brain folds, alveolar membranes, or intestinal epithelium surfaces). Although the present state of knowledge precludes any definitive answers to the ammonoid 'suture problem', future research may benefit from the results presented in this paper.

It should also be noted that spatial development in the analyzed sutures, which is properly quantified by their fractal dimensions, is related to phragmocone size and shape, while the range of self-similarity depends exclusively on phragmocone size. The dissimilar behaviour displayed by X_c and D_f may derive from the morphogenetic mechanism responsible for septal folding throughout the ontogenetic increase of sutural complexity.

As emphasized above, morphometric descriptors for sutures and phragmocones are complexly interrelated. Although bivariate analyses provide valuable information, the topics dealt with in this study will require that multivariate techniques be applied in greater

depth. Future research should also examine phylogenetic relationships among Late Jurassic ammonites.

Acknowledgements. – This research was supported by Projects BTE2001-3029 (MCYT), CGL2004-01615 (MEC) and CGL2005-01316 (MEC), and the Research Groups RNM 146 and RNM 178 Junta de Andalucia, Spain. Thorough editing of the original English manuscript was done by M. Bettini. We gratefully acknowledge constructive comments provided by Ø. Hammer and M. Yacobucci.

References

Ackerly, S.C. 1987: Using 'local' coordinates to analyze shell form in molluscs (abstract). *Geological Society of America Abstracts with Programs 19*, 566.

Ackerly, S.C. 1989: Kinematics of accretionary shell growth, with examples from brachiopods and molluscs. *Paleobiology 15*, 147–164.

Allen, E.G. 2006: New approaches to Fourier analysis of ammonoid sutures and other complex, open curves. *Paleobiology 32*, 299–315.

Almeida, R., Búrquez, A., Curts, J., Dent, M., González-Arreola, C., Hernández, H., Herrera, L., Lazcano-Araujo, A., Martínez, A. & Picones, A. 1974: Descripción morfométrica de ammonites Mexicanos del Jurásico y Cretácico. *Revista de la Sociedad Mexicana de Historia Natural XXXV*, 225–248.

Arkell, W.J., Kummel, B. & Wright, C.W. 1957: Mesozoic Ammonoidea. *In* Moore, R.C. (ed.): *Treatise on Invertebrate Paleontology*. Vol. L, 80–129. Geological Society of America, Boulder, Colorado, and University of Kansas Press, Lawrence, Kansas.

Batt, R.J. 1986: A test of the effects of paleoecological factors on the distribution of ammonite shell morphotypes, Greenhorn cyclothem, Cretaceous western interior seaway. *In* Kauffman, E.G. (ed.): *Cretaceous Biofacies of the Central Part of the Western Interior Seaway: A Field Guidebook. Fourth North American Palaeontogical Convention*, 16–52. The Palaeontological Society, Boulder, Colorado.

Bayer, U. 1977: Cephalopod septa I. Constructional morphology of the ammonite septum. *Neues Jahrbuch für Geologie und Paläontologie Abhandlungen 154*, 19–41.

Bayer, U. 1985: *Pattern Recognition Problems in Geology and Palaeontology*, 229 pp. Springer-Verlag, Berlin.

Bayer, U. & McGhee, G.R. 1984: Iterative evolution of Middle Jurassic ammonite faunas. *Lethaia 17*, 1–16.

Boyajian, G.E. & Lutz, T. 1992: Evolution of biological complexity and its relation to taxonomic longevity in the Ammonoidea. *Geology 20*, 983–986.

Buckman, S.S. 1892: Monograph of the ammonites of the inferior Oolite series. *Palaeontographical Society, London 262*, 456.

Canfield, D.J. & Anstey, R.L. 1981: Harmonic analysis of cephalopod suture patterns. *Mathematical Geology 13*, 23–35.

Chamberlain, J.A. & Westermann, G.E.G. 1976: Hydrodynamic properties of cephalopod shell ornament. *Paleobiology 2*, 316–331.

Chamberlain, J.A., Ward, P.D. & Weaver, J.S. 1981: Post-mortem ascent of *Nautilus* shells: implications for cephalopod paleobiogeography. *Paleobiology 7*, 494–509.

Courville, P., Lang, J. & Thierry J. 1998: Ammonite faunal exchanges between South Tethyan platforms and South Atlantic during the Uppermost Cenomanian-Lowermost/Middle Turonian in the Benue Trough (Nigeria). *Geobios 31*, 187–215.

Cowen, R., Gertman, R. & Wiggett, G. 1973: Camouflage patterns in *Nautilus*, and their implications for cephalopod palaeobiology. *Lethaia 6*, 201–214.

Damiani, G. 1986: Significato funzionale dell'evoluzione dei setti e delle linee di sutura dei nautiliodi e degli ammonoidi. *In* Pallini, G. (ed.): *Atti I Convengo Internationale: Fossili, Evoluzione, Ambiente*, 123–130. Tecnoscienza, Pergola, Rome, Italy.

Daniel, T.L., Helmuth, B.S., Saunders, W.B. & Ward, P. 1997: Septal complexity in ammonoid cephalopods increased mechanical risk and limited depth. *Paleobiology 23*, 470–481.

Davis, J.C. 1986: *Statistics and Data Analysis in Geology*, 2nd edn. John Wiley & Sons, New York.

Dommergues, J.L. 1990: Ammonoids. *In* Mc-Namara, K.J. (ed.): *Evolutionary Trends*, 162–187. Belhaven Press, London.

Dommergues, J.L., Laurin, B. & Meister, C. 1996: Evolution of ammonoid morphospace during the early Jurassic radiation. *Paleobiology 22*, 219–240.

Donovan, D.T. 1994: Evolution in some early Jurassic ammonites: Asteroceratinae, Oxynoceratidae and related forms. *Palaeopelagos Special Publication 1, Roma. Proceedings of the 3rd Pergola International Symposium 'Fossili, Evoluzione, Ambiente'*, 383–396. CSA Università 'La Sapienza', Roma.

Ehrlich, R. & Weinberg, B. 1970: An exact method for characterization of grain shape. *Journal of Sedimentary Petrology 40*, 205–212.

Fisher, D.C. 1986: Progress in organismal design. *In* Raup, D. & Jablonski, D. (eds): *Patterns and Processes in the History of Life*, 99–117. Springer-Verlag, Berlin.

García-Ruiz, J.M., Checa, A. & Rivas, P. 1990: On the origin of ammonoid sutures. *Paleobiology 16*, 349–354.

Gildner, R.F. 2003: A Fourier method to describe and compare suture patterns. *Palaeontologia Electronica 6*, 12. http://palaeo-electronica.org/palaeo/2003_1/suture/issue1_03.htm

Gould, S.J., 1988: On replacing the idea of progress with an operational notion of directionality. *In* Nitecki, M.H. (ed.): *Evolutionary Progress*, 319–338. University of Chicago Press, Chicago.

Gould, S.J., 1996: *Full House*. Harmony, New York.

Guex, J., Koch, A., O'Dogherty, L. & Bucher, H. 2003: A morphogenetic explanation of Buckman's law of covariation. *Bulletin de la Société Géologique de France 174*, 603–606.

Haas, O. 1942: Recurrence of morphologic types and evolutionary cycles in Mesozoic ammonites. *Journal of Paleontology 16*, 643–650.

Hammer, Ø. & Bucher, H. 2005: Buckman's first law of covariation – a case of proportionality. *Lethaia 38*, 67–72.

Hassan, M.A., Westermann, G.E.G., Hewitt, R.A. & Dokainish, M.A. 2002: Finite-element analysis of simulated ammonoid septa (extinct Cephalopoda): septal and sutural complexities do not reduce strength. *Paleobiology 28*, 113–126.

Hewitt, R.A. & Westermann, G.E.G. 1987: Function of complexly fluted septa in ammonoid shells II. Septal evolution and conclusions. *Neues Jahrbuch für Geologie und Paläontologie Abhandlungen 174*, 135–169.

Hewitt, R.A. & Westermann, G.E.G. 1997: Mechanical significance of ammonoid septa with complex sutures. *Lethaia 30*, 205–212.

Illert, C. 1987: Formulation and solution of the classical problem. I. Shell geometry. *Nuovo Cimento 9*, 791–813.

Illert, C. 1989: Formulation and solution of the classical problem. II. Tubular three-dimensional seashell surfaces. *Nuovo Cimento 11*, 761–780.

Kennedy, W.J. & Cobban, W.A. 1976: Aspects of ammonite biology, biogeography, and biostratigraphy. *Special Papers in Palaeontology 17*, 1–94.

Kröger, B. 2002: On the efficiency of the buoyancy apparatus in ammonoids: evidences from sublethal shell injuries. *Lethaia 35*, 61–70.

Kulicki, C. 1979: The ammonite shell: its structure, development and biological significance. *Palaeontologica Polonica 39*, 79–142.

Kulicki, C. & Mutvei, H. 1988: Functional interpretation of ammonoid septa. *In* Pietronero, L. & Tosati, E. (eds): *Fractals In Physics*, 177–180. North-Holland, Amsterdam.

Kullmann, J. & Wiedmann, J. 1970: Significance of sutures in phylogeny of Ammonoidea. *The University of Kansas Palaeontological Contributions 47*, 1–32.

Landman, N.H. 1988: Heterochrony in ammonites. *In* McKinney, M.L. (ed.): *Heterochrony in Evolution: A Multidisciplinary Approach*, 159–182. Plenum, New York.

Lewy, Z. 2002: The function of the ammonite fluted septal margins. *Journal of Paleontology 76*, 63–69.

Lohmann, G.P. 1983: Eigenshape analysis of microfossils: A general morphometric procedure for describing changes in shape. *Mathematical Geology 15*, 659–672.

Lohmann, G.P. & Schweitzer, P.N. 1990: On eigenshape analysis. *In* Rolf, F.J. & Bookstein F.L. (eds): *Proceedings of the Michigan Morphometrics Workshop*. 147–166. University of Michigan Museum of Zoology, Special Publication no. 2, Michigan.

Long, C.A. 1985: Intricate sutures as fractal curves. *Journal of Morphology 185*, 285–295.

Lutz, T.M. & Boyajian, G.E. 1995: Fractal geometry of ammonoid sutures. *Paleobiology 21*, 329–342.

MacLeod, N. 1999: Generalizing and extending the eigenshape method of shape space visualization and analysis. *Paleobiology 25*, 107–138.

Maeda, H. & Seilacher, A., 1996: Ammonoid taphonomy. *In* Landman, N.H., Tanabe, K., Davis, R.A. (eds): *Ammonoid Paleobiology*, 543–578. Plenum, New York.

Mandelbrot, B. 1983: *The Fractal Geometry of Nature*. 2nd edn. W.H. Freeman and Company, New York.

Mapes, R.H., Tanabe, K. & Landman H. 1999: Siphuncular membranes in Upper Palaeozoic prolecanitid ammonoids from Nevada, USA. *In* Histon, K. (ed.) *V International Symposium Cephalopods – Present and Pas*. Abstract Volume, 83 pp. *Berichte der Geologischen Bundesanstalt 46*. Vienna, Austria.

McGowan, A.J. 2004: The effect of the Permo-Triassic bottleneck on Triassic ammonoid morphological evolution. *Paleobiology 30*, 369–395.

McShea, D.W. 1991: Complexity and evolution: what every-one knows. *Biology and Philosophy 6*, 303–324.

Newell, N. 1949: Phyletic size increase, an important trend illustrated by fossil invertebrates. *Evolution 3*, 103–124.

Okamoto, T. 1984: Theoretical morphology of *Nipponites* (a heteromorph ammonoid). *Fossil (Kaseki), Palaeontological Society of Japan 36*, 37–51 (in Japanese).

Okamoto, T. 1986: Analysis of morphology in heteromorph ammonites. *Annual Meeting of the Palaeontological Society of Japan 1986*, *Abstracts with Program*, 34 pp. (in Japanese).

Okamoto, T. 1988: Analysis of heteromorph ammonoids by differential geometry. *Palaeontology 31*, 37–51.

Okamoto, T. 1996: Theoretical modeling of ammonoid morphology. *In* Landman, N.H., Tanabe, K. & Davis, A. (eds): *Ammonoid Paleobiology*. *Topics in Geobiology*, *13*, 225–251. Plenum Press, New York.

Olóriz, F. & Palmqvist, P. 1995: Sutural complexity and bathymetry in ammonites: fact or artifact? *Lethaia 28*, 167–170.

Olóriz, F., Palmqvist, P. & Pérez-Claros, J.A. 1997: Shell features, main colonized environments, and fractal analysis of sutures in Late Jurassic ammonites. *Lethaia 30*, 191–204.

Olóriz, F., Palmqvist, P. & Pérez-Claros, J.A. 1999: Recent advances in morphometric approaches to covariation of shell features and the complexity of suture lines in late Jurassic ammonites, with references to the major environments colonized. *In* Olóriz, F. & Rodríguez-Tovar, F.J. (eds): *Advancing Research on Living and Fossil Cephalopods*, 273–293. Plenum Press, New York.

Olóriz, F., Palmqvist, P. & Pérez-Claros, J.A. 2002: Morphostructural constraints and phylogenetic overprint on sutural frilling in Late Jurassic ammonites. *Lethaia 35*, 158–168.

Palmqvist, P. 1989: Análisis del crecimiento y la forma en los foraminíferos planctónicos, con fines biométricos. Unpublished PhD Thesis, University of Málaga, Spain, 296 pp.

Palmqvist, P., Gibert, J., Pérez-Claros, J.A. & Santamaría, J.L. 1996: Comparative morphometric study of a human phalanx from the lower Pleistocene site at Cueva Victoria (Murcia, Spain), by means of Fourier analysis, shape coordinates of landmarks, principal and relative warps. *Journal of Archaeological Science 23*, 95–107.

Pérez-Claros, J.A. 1999: Análisis morfométrico de la complejidad sutural en ammonites del Jurásico superior, en relación a las características del fragmocono y el paleoambiente. Unpublished PhD Thesis, Universidad de Málaga, Spain, 509 pp.

Pérez-Claros, J.A. 2005: Allometric and fractal exponents indicate a connection between metabolism and complex septa in ammonites. *Paleobiology 31(2)*, 221–232.

Pérez-Claros, J.A., Palmqvist, P. & Olóriz, F. 2002: First and second order levels of suture complexity in ammonites: a new methodological approach using fractal analysis. *Mathematical Geology 34(3)*, 323–343.

Raup, D.M. 1966: Geometric analysis of shell coiling: general problems. *Journal of Paleontology 40*, 1178–1190.

Raup, D.M. 1967: Geometric analysis of shell coiling: coiling in ammonoids. *Journal of Paleontology 41*, 43–65.

Raup, D.M. & Stanley, S. 1971: Principles of Invertebrate Paleontology. 388 pp. Freeman, San Francisco, California.

Rice, S.H. 1998: The biogeometry of mollusc shells. *Paleobiology 24*, 133–149.

Rohlf, F.J. 1990: Fitting curves to outlines. *In* Rolf, F.J. & Bookstein F.L. (eds): *Proceedings of the Michigan Morphometrics Workshop*, 167–179. University of Michigan Museum of Zoology, Special Publication no. 2, Ann Arbor, Michigan.

Saunders, W.B. 1995: The ammonoid suture problem: relationships between shell and septum thickness and suture complexity in Paleozoic ammonoids. *Paleobiology 21*, 343–355.

Saunders, W.B. & Swan, A.R.H. 1984: Morphology and morphologic diversity of mid-Carboniferous (Namurian) ammonoids in time and space. *Paleobiology 10*, 195–228.

Saunders, W.B. & Work, D.M. 1996: Shell morphology and suture complexity in Upper Carboniferous ammonoids. *Paleobiology 22*, 189–218.

Saunders, W.B. & Work, D.M. 1997: Evolution of shell morphology and suture complexity in Paleozoic prolecanitids, the rootstock of Mesozoic ammonoids. *Paleobiology 23*, 301–325.

Saunders, W.B., Work, D.M. & Nikolaeva, S.V. 1999: Evolution of complexity in Paleozoic ammonoid sutures. *Science 288*, 760–763.

Saunders, W.B., Work, D.M. & Nikolaeva, S.V. 2004: The evolutionary history of shell geometry in Paleozoic ammonoids. *Paleobiology 30*, 19–43.

Schindewolf, O.H. 1968: Analyse einen Ammoniten-Gehauses. *Akademie der Wissenschaften und der Literatur in Mainz Abhandlungen der Mathematisch-Naturwissenschaftlichen Klasse 8*, 139–188.

Seilacher, A. 1988: Why are nautiloid and ammonite sutures so different? *Neues Jahrbuch für Geologie und Paläontologie Abhandlungen 177*, 41–69.

Stanley, S.M. 1973: An explanation for Cope's rule. *Evolution 27*, 1–26.

Stone, J.R. 1995: Cerioshell: a computer program designed to simulate variation in shell form. *Paleobiology 21*, 509–519.

Straney, D.O. 1990: Median axis methods in morphometrics. *In* Rolf, F.J. & Bookstein F.L. (eds): *Proceedings of the Michigan Morphometrics Workshop*. 147–166. University of Michigan Museum of Zoology, Special Publication no. 2, Ann Arbor, Michigan.

Tanabe, K., Mapes, R.H., Sasaki, T. & Landman, N.H. 2000: Soft-part anatomy of the siphuncle in Permian prolecanitid ammonoids. *Lethaia 33*, 83–91.

Ward, P.D. 1980: Comparative shell shape distributions in Jurassic-Cretaceous ammonites and Jurassic-Tertiary nautiloids. *Paleobiology 6*, 32–43.

Ward, P.D. 1981: Shell sculpture as defensive adaptation in ammonoids. *Paleobiology 7*, 96–100.

Ward, P.D. 1987: *The Natural History of Nautilus*. Allen and Unwin, London.

Weitschat, W. & Bandel, K. 1991: Organic components in phragmocones of Boreal Triassic ammonoids: implications for ammonoid biology. *Paläontologische Zeitschrift 65*, 269–303.

Westermann, G.E.G. 1966: Covariation and taxonomy of the Jurassic ammonite *Sonninia adrica* (Waagen). *Neues Jahrbuch für Geologie und Paläontologie Abhandlungen 124*, 289–312.

Westermann, G.E.G. 1971: Form, structure and function of shell and siphuncle in coiled Mesozoic ammonoids. *Royal Ontario Museum, Life Sciences Contributions 78*, 1–39.

Yacobucci, M.M. 2004: Buckman's paradox: variability and constraints on ammonoid ornament and shell shape. *Lethaia 37*, 57–69.